

Lawrence Berkeley National Laboratory

Recent Work

Title

THE INFLUENCE OF SURFACE TURBULENCE AND SURFACTANTS ON GAS TRANSPORT THROUGH LIQUID INTERFACES

Permalink

<https://escholarship.org/uc/item/8b8916pq>

Authors

Springer, Thomas G.
Pigford, Robert L.

Publication Date

1969-10-01

C.2

THE INFLUENCE OF SURFACE TURBULENCE AND SURFACTANTS
ON GAS TRANSPORT THROUGH LIQUID INTERFACES

RECEIVED
LAWRENCE

RADIATION LABORATORY Thomas G. Springer and Robert L. Pigford

JAN 6 1970

October 1969

LIBRARY AND
DOCUMENTS SECTION

AEC Contract No. W-7405-eng-48

TWO-WEEK LOAN COPY

*This is a Library Circulating Copy
which may be borrowed for two weeks.
For a personal retention copy, call
Tech. Info. Division, Ext. 5545*

LAWRENCE RADIATION LABORATORY
UNIVERSITY of CALIFORNIA BERKELEY

UCRL-18993

DISCLAIMER

This document was prepared as an account of work sponsored by the United States Government. While this document is believed to contain correct information, neither the United States Government nor any agency thereof, nor the Regents of the University of California, nor any of their employees, makes any warranty, express or implied, or assumes any legal responsibility for the accuracy, completeness, or usefulness of any information, apparatus, product, or process disclosed, or represents that its use would not infringe privately owned rights. Reference herein to any specific commercial product, process, or service by its trade name, trademark, manufacturer, or otherwise, does not necessarily constitute or imply its endorsement, recommendation, or favoring by the United States Government or any agency thereof, or the Regents of the University of California. The views and opinions of authors expressed herein do not necessarily state or reflect those of the United States Government or any agency thereof or the Regents of the University of California.

THE INFLUENCE OF SURFACE TURBULENCE AND SURFACTANTS
ON GAS TRANSPORT THROUGH LIQUID INTERFACES*

Thomas G. Springer[†] and Robert L. Pigford

Department of Chemical Engineering
and Lawrence Radiation Laboratory
University of California
Berkeley, California 94720

October 1969

ABSTRACT

A new experimental technique is used to measure the effects of surface turbulence and surfactants on mass transfer rates at gas-liquid interfaces. Results indicate that at high turbulence rates the statistical nature of interfaces, with and without surfactants present, may be described by a Danckwerts-type distribution function of surface ages. Measurements of surface film mass transfer resistances show that soluble surfactants offer no measurable resistance while insoluble films show definite resistance to passage of gas molecules. The nature of surface films and their stability in the presence of interfacial turbulence is discussed.

* Work performed under the auspices of the U. S. Atomic Energy Commission.

[†] Present address: E. I. du Pont de Nemours and Co., Wilmington, Delaware.

INTRODUCTION

There has been a large amount of work in recent years studying the interfacial mass transfer resistance of surfactant films, but the more important problem of characterization of the fluid motion at turbulent interfaces with and without surface films present has not received attention. Bussey (1966) showed the presence of soluble surfactants adds no measurable resistance to mass transfer through water interfaces. It is also known that insoluble materials such as 1-hexadecanol when spread as a monolayer on water can add an additional resistance to mass transfer through the interface (Plevan and Quinn, 1965), (Sada and Himmelblau, 1967), but the effects of surface films on interfacial mobility during turbulent mixing of the liquid are not known. It has been postulated (Davies, 1964) that possible hydrodynamic effects of surface films cause damping of eddies as they approach the interface and reduce mass transfer rates.

An experimental technique has been described (Lamb et al., 1969) for the observation of the resistance to passage of a soluble gas through a gas-liquid interface under dynamic conditions using frequency response analysis. From the data of the experiment one may test various interface mass transfer mechanisms.

The experimental apparatus, called an interface impedance bridge, is comprised of two chambers, each consisting of a variable-volume gas space with a deep pool of liquid below. One chamber has provisions for varying the surface conditions of the liquid; the second chamber is used as a reference chamber of calculable impedance. The gas pressure may

be varied in the two chambers simultaneously in a sinusoidal manner. From the measured frequency response of the bridge-type apparatus one can calculate the impedance of the test chamber and relate the impedance to resistances to mass transfer at the gas-liquid interface.

Characterization of the mass transfer coefficient for a randomly turbulent surface, following the suggestion of Danckwerts (1951) for example, may be examined since the frequency response information yields the whole statistical distribution of fluid particle residence times in the interface as well as the average surface element age and replacement frequency.

One may also examine the effect of surface films, both soluble and insoluble, on mass transfer through a stagnant interface as well as a turbulent interface. These measurements allow one to separate the surface resistance and hydrodynamic effects of films to determine their independent effects.

QUANTITATIVE DEVELOPMENT

1. Statistical Characteristics of Turbulent Interfaces

Comparison of pressure oscillations, occurring in two chambers each containing a soluble gas above deep pools of liquid, caused by sinusoidal volume changes yields (Lamb et al., 1969)

$$\frac{\hat{p}_1 - \hat{p}_2}{\hat{p}_2} = \frac{\hat{\Delta p}}{\hat{p}_2} = \frac{Q_2 k_{L2}(\omega) - Q_1 k_{L1}(\omega)}{i\omega + Q_1 k_{L1}(\omega)} \quad (1)$$

with $Q = H A T_0 / V_0$, where H is the Henry's Law coefficient, A is the

known area of the interface, $k_L(\omega)$ is the possibly frequency-dependent mass transfer coefficient of the liquid surface, T_0 is the time-average surrounding temperature and V_0 is the average gas volume of the chambers. \hat{p} is the amplitude of the pressure oscillations and $\hat{\Delta p}$ is that of the pressure difference signal.

Experimentally one may use either an impermeable surface or a stagnant, clean liquid surface for a standard interface of calculable impedance. Indeed, in our experimental work both types of reference chambers have been used. However, it is slightly more convenient mathematically to use an impermeable surface as the standard reference. Since it has been shown (Lamb et al., 1969) that the behavior of a clean, stagnant interface can be calculated reliably, it is a simple matter to convert from one standard reference to the other. For the sake of brevity the quantitative analysis presented here will deal with an impermeable surface as a reference.

Assume that in chamber two a turbulent interface exists, obtained by stirring a pool of clean liquid, and that an impermeable interface exists in the reference chamber. Equation (1) then becomes

$$\frac{\hat{\Delta p}}{\hat{p}_t} = \frac{Q_t k_{Lt}(\omega)}{i\omega} \quad (2)$$

Measurement of the indicated pressure and pressure-difference signals enables one to calculate the frequency-dependent mass transfer coefficient, $k_{Lt}(\omega)$.

To find the flux through a turbulent interface one must make some assumptions concerning the nature of the interfacial fluid motion. As a first approximation a randomly turbulent surface may be assumed, following the suggestion of Danckwerts (1951). He assumed that a turbulent interface consists of a mosaic of elements of varying ages, which are randomly replaced by fresh elements from the bulk of the liquid. Following this assumption, let

$f(\theta)$ = surface age distribution function

$f(\theta)d\theta$ = fraction of the interface which is occupied by particles which have been exposed there for a time, θ , within time increment, $d\theta$.

By definition

$$\int_0^{\infty} f(\theta)d\theta = 1 .$$

If one assumes that the scale of turbulence is much greater than the depth of penetration of the solute diffusing from the surface, one may apply the transient diffusion equation to each surface element independently.

Let α = time when an element was first exposed at the surface.

Then $\theta = t - \alpha$ = the age of the surface element and

$$\mathcal{D} \left(\frac{\partial^2 c}{\partial x^2} \right) = \frac{\partial c}{\partial t} \quad \text{for } t \geq \alpha, x \geq 0 . \quad (3)$$

The boundary conditions on $c(x, \theta)$ are,

$$c(0, \theta) = H \hat{p} \exp(i\omega t) = H \hat{p} \exp(i\omega \alpha) \exp(i\omega \theta)$$

$$c(\infty, 0) = c(x, 0) = 0$$

Laplace transforms may be used to solve Eq. (3) subject to the listed boundary conditions. The solution is

$$\bar{c}(x, m) = H \hat{p} \left(\frac{1}{m - i\omega} \right) \exp(i\omega \alpha - \left(\frac{m}{\mathcal{D}} \right)^{1/2} x) \quad (4)$$

where m represents the Laplace transform variable and x is the distance from the interface. The Laplace transform of the flux at the interface may be found from Eq. (4).

$$L(\dot{n}) = AH \hat{p} \mathcal{D}^{1/2} \left(\frac{m^{1/2}}{m - i\omega} \right) \exp(i\omega \alpha) \quad (5)$$

where n represents the instantaneous number of moles of gas above the liquid and the dot above represents differentiation with respect to time. The inverse transform (Erdelyi, 1954) of Eq. (5) is

$$\dot{n}(\theta, t) = AH \hat{p} \exp(i\omega t) (\mathcal{D} / \pi \theta)^{1/2} [\exp(i\omega \theta) + (i\omega \mathcal{D})^{1/2} \text{erf}(i\omega \theta)^{1/2}] \quad (6)$$

The average, steady state rate of absorption into the turbulent interface of age distribution $f(\theta)$ may be found by summation over all surface elements

$$\dot{n}(t) = \int_0^{\infty} \dot{n}(t, \theta) f(\theta) d\theta \quad (7)$$

This gives

$$\dot{n}(t) = HA \hat{p} \exp(i\omega t) G(\omega) \quad (8)$$

where

$$G(\omega) = (\mathcal{D}/\pi)^{1/2} \int_0^{\infty} \left[f(\theta) + i\omega \int_{\theta}^{\infty} f(x) dx \right] \theta^{-1/2} \exp(-i\omega\theta) d\theta \quad (9)$$

A mass balance at the liquid interface yields

$$\dot{n}(t) = -Hk_{Lt}(\omega) A(p-p_0) = -\mathcal{D}A \left(\frac{\partial c}{\partial x} \right) \Big|_{x=0} \quad (10)$$

where $p = p_0 + \hat{p} \exp(i\omega t)$.

Using Eqs. (8) and (10), one can see that

$$k_{Lt}(\omega) = G(\omega) \quad (11)$$

It is obvious that knowledge of $f(\theta)$ allows calculation of the mass transfer coefficient for a turbulent interface. Conversely, since one can determine $k_{Lt}(\omega)$ experimentally, $f(\theta)$ can be found from measured values of $k_{Lt}(\omega)$ or $G(\omega)$ if Eq. (9) can be solved as an integral equation for the unknown function, $f(\theta)$.

Consider the integral Eq. (9) and note that we are free to define $f(\theta) = 0$ for $\theta < 0$. Thus

$$\int_{\theta}^{\infty} f(x) dx = 1 \quad \text{for } \theta \leq 0 .$$

The integral over the full range of θ is

$$G^*(\omega) = \left(\frac{2}{\pi}\right)^{1/2} \int_{-\infty}^{\infty} \left[f(\theta) + i\omega \int_{\theta}^{\infty} f(x) dx \right] \theta^{-1/2} \exp(-i\omega\theta) d\theta \tag{12}$$

$$G^*(\omega) = \left(\frac{2}{\pi}\right)^{1/2} \int_{-\infty}^0 i\omega \theta^{-1/2} \exp(-i\omega\theta) d\theta + G(\omega) .$$

Evaluation of the first integral gives

$$G^*(\omega) = (i\omega \mathcal{D})^{1/2} + G(\omega) .$$

Consider now solving Eq. (12) to find $f(\theta)$. The second part of the integral in Eq. (12) can be integrated by parts. Combining the result with Eqs. (11) and (12) gives

$$G^*(\omega) = -\frac{1}{2} \left(\frac{2}{\pi}\right)^{1/2} \int_{-\infty}^{\infty} \theta^{-3/2} \int_{\theta}^{\infty} f(x) dx \exp(-i\omega\theta) d\theta . \tag{13}$$

This is in the form of a Fourier integral, and, subject to certain continuity conditions, it follows that

$$\int_{\theta}^{\infty} f(x)dx = -\left(\frac{\theta^3}{2\pi}\right)^{1/2} \int_{-\infty}^{\infty} \exp(i\omega\theta)[G(\omega) + (i\omega 2)^{1/2}]d\omega \quad (14)$$

Differentiation gives

$$f(\theta) = (1/2)(\pi 2)^{-1/2} \int_{-\infty}^{\infty} (3\theta^{1/2} + 2i\omega\theta^{3/2})[G(\omega) + (i\omega 2)^{1/2}] \exp(i\omega\theta)d\omega \quad (15)$$

Equation (15) requires the observation of $G(\omega)$ over both positive and negative frequencies. The negative range is obviously impossible to observe experimentally. Fortunately, however, the fact that the distribution function $f(\theta)$ is real makes it possible to show that the real part, $R(\omega)$, of the observed frequency response is an even function of ω while the imaginary part, $I(\omega)$, is odd. After some algebra, Eq. (15) can be shown to be equivalent to

$$f(\theta) = (\theta/\pi 2)^{1/2} \int_0^{\infty} [(3R - 2\omega\theta I)\cos(\omega\theta) - (3I + 2\omega\theta R)\sin(\omega\theta)]d\omega \quad (16)$$

which is the form most suitable for numerical evaluation. For details on how to do this, see Springer (1969).

2. Frequency Response of Interface Models

a. The Randomly Turbulent Interface

Using the previous analysis one may test models concerning the structure of a turbulent interface by comparison of an observed frequency

response with one which has been predicted. Many surface renewal models have been postulated, but one of the earliest and simplest of these theories was proposed by Danckwerts (1951). He assumed that the motion of a stirred liquid will continually replace with fresh fluid those elements which have been exposed for a finite length of time. Danckwerts, also assumed that the chance of an element of surface being replaced within a given time is independent of its age; hence, the fractional rate of replacement of the elements belonging to every age group is equal to a constant s . According to these assumptions,

$$f(\theta) = s \exp(-s\theta) \quad (17)$$

Calculation of the frequency response behavior of such a surface by using Eqs. (2), (9), (11) and (17) yields

$$\frac{\hat{\Delta p}}{\hat{p}_t} = Q\omega^{1/2} [(s^2 + \omega^2)^{1/4} / \omega] \angle \tan^{-1} \left[\frac{(s^2 + \omega^2)^{1/2} + s}{(s^2 + \omega^2)^{1/2} - s} \right]^{1/2} \quad (18)$$

From preliminary results by Lamb (1965) it appeared that frequency response results would be similar to those predicted by the Danckwerts model. For this reason, it was decided that this model would be used as a trial basis for evaluating new data. The phase and amplitude data may be analyzed separately, according to Eq. (18), to determine best-fit values for the constants Q and s . For convenience let $|\hat{\Delta p} / \hat{p}_t| = A(\omega)$ and represent the phase angle by $\phi(\omega)$. Using the amplitude results in the following form

$$(\omega A)^4 = Q \mathcal{D}^{1/2} s^2 + Q \mathcal{D}^{1/2} \omega^2 \quad (19)$$

and the phase in the form

$$2 \tan \phi / (\tan^2 \phi - 1) = \omega / s \quad (20)$$

one may apply a linear least squares analysis to collected data as shown in Eqs. (19) and (20) to find Q and s . One can then graphically compare the observed frequency response, according to Eq. (2), with that from Eq. (18).

b. Film-Covered Liquid Surfaces

Consider next a stagnant liquid covered with a thin surface film. Transport of gas through the interface is described by the following equation and boundary conditions

$$\mathcal{D} \frac{\partial^2 c}{\partial x^2} = \frac{\partial c}{\partial t}$$

$$c(\infty, t) = c_o = H p_o$$

$$N(t) = - \mathcal{D} \frac{\partial c(0, t)}{\partial x} = K_f [H p(t) - c(0, t)]$$

Assume a solution of the form

$$c(x, t) = \hat{c}(x) \exp(i\omega t) + H p_o$$

and remember that

$$p(t) = p_0 + \hat{p} \exp(i\omega t) .$$

Let $N = \hat{N} \exp(i\omega t)$, then

$$\hat{N} = \frac{K_f (i\omega \mathcal{D})^{1/2}}{K_f + (i\omega \mathcal{D})^{1/2}} H \hat{p} .$$

Consider an interface impedance bridge where in the test chamber there is a stagnant liquid covered with a surface film and where the standard reference chamber is an impermeable surface. The pressure-difference signal from such a bridge may be found knowing the flux across the interface, N_0 .

$$\frac{\hat{p}_I - \hat{p}_f}{\hat{p}_f} = Q_f \frac{K_f (i\omega \mathcal{D})^{1/2}}{i\omega (K_f + (i\omega \mathcal{D})^{1/2})} . \quad (21)$$

The subscript f indicates that a film-covered surface is present in that chamber; I denotes a chamber containing an impermeable surface.

One may rearrange the above equation so that a linear least squares analysis may be applied to observed pressure signals to obtain the surface film coefficient K_f . One may recognize that K_f must be a real number to be physically realizable and therefore use only the real part of Eq. (21).

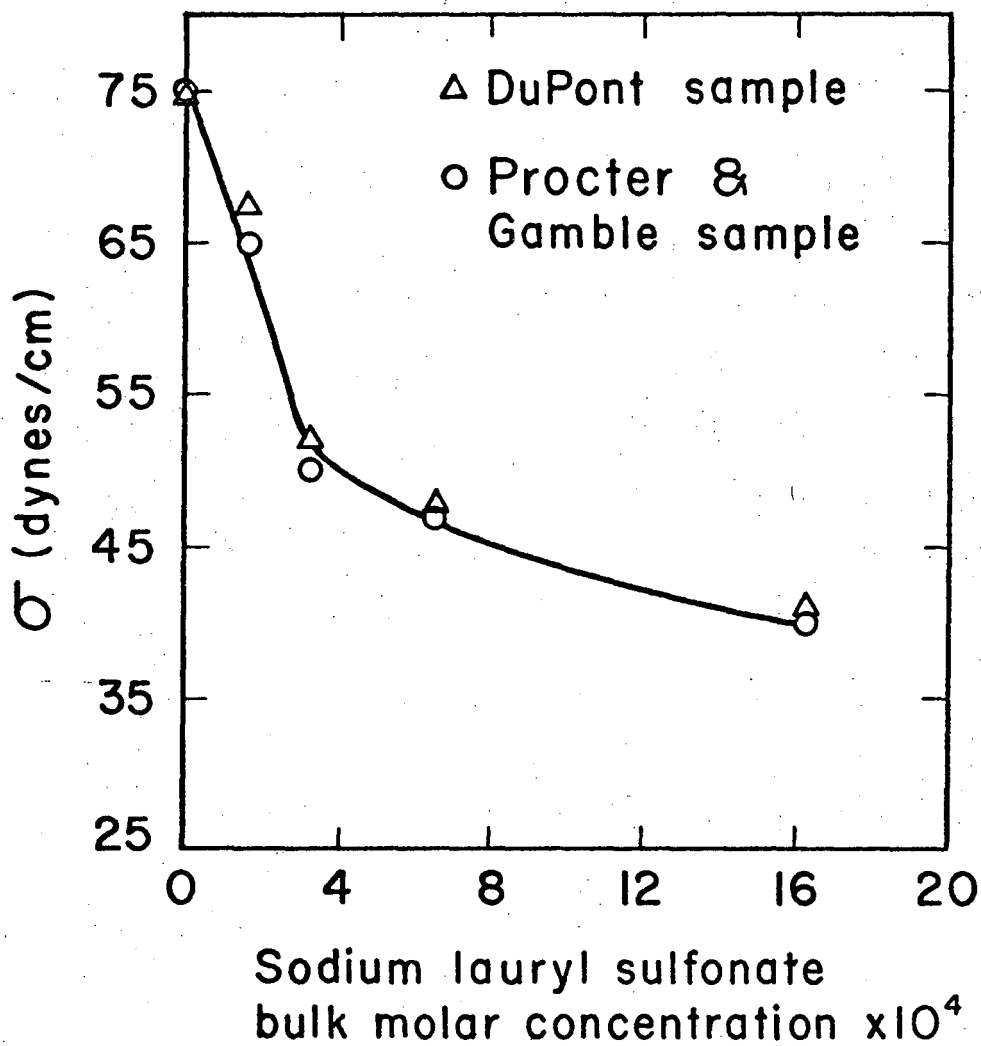
Thus it is clear that, using the frequency response data, one can obtain both statistical distributions and physical constants for specific models.

MATERIALS

In this work the gas-liquid system used was sulfur dioxide-water. An anhydrous grade (99.90% purity by weight) sulfur dioxide was obtained from the Matheson Company. The water used in the experiments was distilled water, from a laboratory supply, that had been degassed and stored under a sulfur dioxide atmosphere.

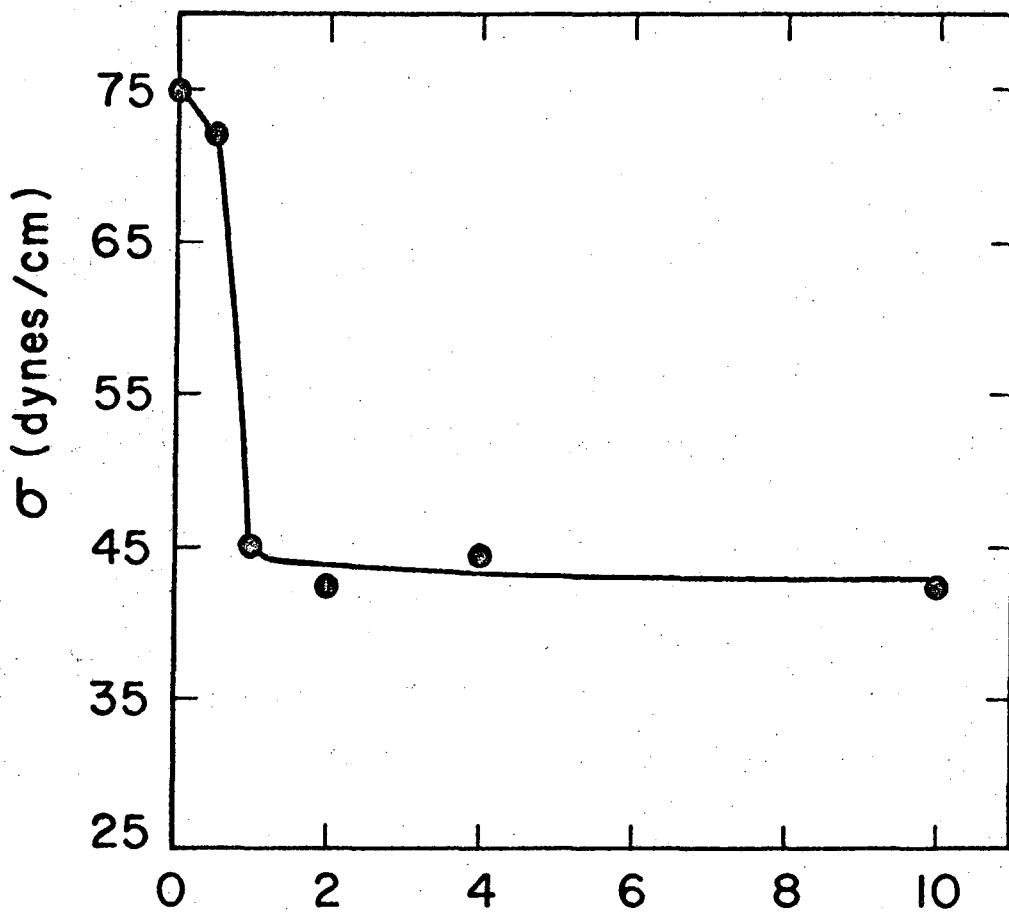
Two surfactants were used. They were 1-hexadecanol (cetyl alcohol) and sodium lauryl sulfonate. The insoluble surfactant, 1-hexadecanol, was obtained from Eastman Chemicals Company and was reported to be a reagent grade. The soluble surfactant, sodium lauryl sulfonate, was obtained from two sources, Procter and Gamble and E. I. du Pont de Nemours Company. The sample from Du Pont was of questionable purity, but the sample from Procter and Gamble was reported to be 99⁺% pure.

No attempt was made to purify samples further, but as criteria for performance surface tension-versus-concentration curves were measured. A cenco Du Nouy (ring-type) Tensiometer was used to measure surface tension; the results are shown in Figs. 1 and 2. Note that, despite the unknown purity for the sample obtained from Du Pont, its curve in Fig. 1 agrees very well with the curve obtained with the carefully purified sample from Procter and Gamble, indicating that surface-active impurities must have been negligible. Note also that the concentration of 1-hexadecanol is given in monolayers present on the surface. They were calculated assuming that a single molecule occupies 20 sq Angstroms of the surface.



XBL6910-3915

Fig. 1.



Surface concentration of 1-hexadecanol
in equivalent monolayers

XBL6910-3916

Fig. 2.

The liquid surfaces in all tests were initially cleaned by placing a clean absorbent filter paper on the surface to remove dust particles and any insoluble contaminants that might have collected there.

It was found that the insoluble surfactant was best spread by pipetting an ether solution onto a liquid surface contained in a small movable cup. The solvent was allowed to evaporate and the cup was attached to the inside of the test chamber lid. The surfactant was added to the surface by immersing the cup under the water in the closed chamber. The soluble surfactant was added by use of the cup also, but no solvent or liquid was added to the cup. For complete details of the cleaning procedure and the method of surfactant addition see Springer (1969).

EXPERIMENTAL RESULTS

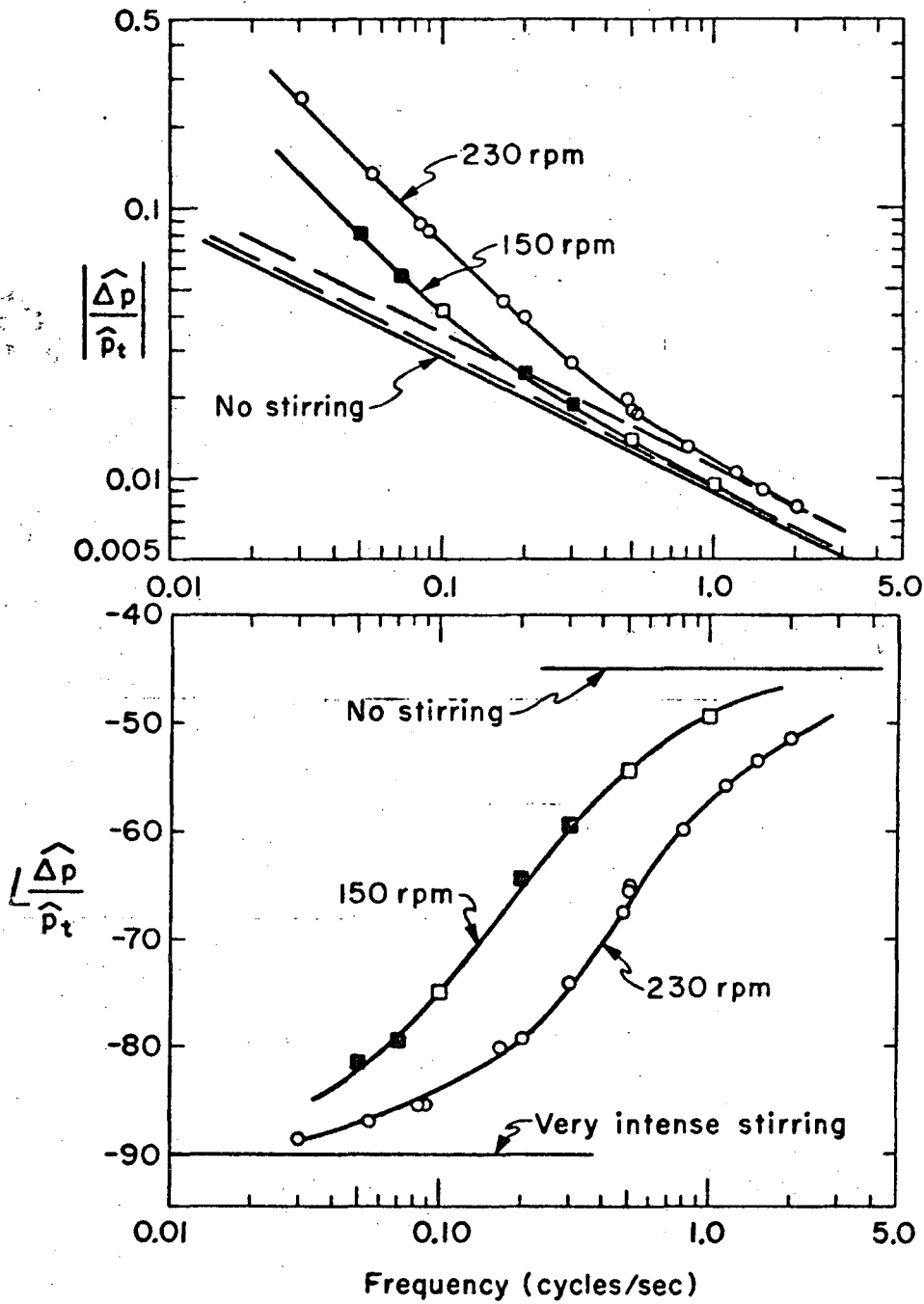
Before results are given, the procedure for presentation of data needs to be explained. As noted earlier, it is possible for frequency response to be measured relative to either an impermeable surface or a stagnant liquid surface as standards in the reference chamber. Data were taken in both ways, but were presented relative to an impermeable surface in results shown here. To distinguish between methods of measurements, all data points taken relative to an impermeable surface are shown as darkened symbols; those taken relative to a stagnant liquid interface are shown as open symbols on the graphs.

It has also been shown earlier that data may be analyzed by treating the amplitude and phase data results separately. The data

shown for clean, turbulent interfaces includes plots of both amplitude and phase relationships. These plots are typical of other results, so to conserve space only the amplitude results will be plotted for other data. The tables containing results of analysis of data will contain results for both amplitude and phase data. Complete tables of all pertinent data have been deposited as Document No. 0000 with the ADI Auxiliary Publications Project, Photoduplication Service, Library of Congress, Washington, D. C. 20540, where copies may be secured.

1. Clean Turbulent Surfaces

Consider a turbulent, clean interface, obtained by stirring the pool of liquid below at a rate of 230 rpm. By comparing this interface with an impermeable one in a standard reference chamber using the interface impedance bridge, the frequency response shown in Fig. 3 was obtained. The solid curved line represents the response predicted by Eq. (18) using the values of s and $Q^* = Q \mathcal{D}^{1/2}$ given in Table I; the straight line is the theoretical response of a clean, stagnant surface compared to an impermeable surface. Note that as frequency becomes large the response of a turbulent interface should approach that of a stagnant interface. Introduction of turbulence to a stagnant interface causes an increase in the surface area for mass transfer because of ripples produced in the otherwise smooth surface and also because of wetting of the chamber wall directly above the normal liquid level due to the irregular motion of the surface. The apparent increase is shown by the values of Q^* listed in Table I. The dashed lines in Fig. 3 represent the theoretical response of a stagnant surface of surface area



XBL6910-3913

Fig. 3.

Table I. Results of least squares analysis of data for a clean, turbulent interface.

Stirring Speed rpm	Phase Data		Amplitude Data
	s, sec ⁻¹	s, sec ⁻¹	Q*, cm ⁻¹
0	0	0	0
150	1.04±0.07 ^a	1.09±0.08	0.0233±0.00007
230	2.88±0.09	2.87±0.16	0.0272±0.00011

^aStandard error computed on the basis of 95% confidence level, i.e. approximately two standard deviations.

equivalent to the turbulent interface. Based on the surface area of the stagnant pool of liquid (625 cc), a gas-space average volume of 4500 cc, a Henry's Law coefficient of 0.02368 g-moles/(cc)(atm), and a diffusivity in water of 0.0000146 sq cm/sec for dissolved sulfur dioxide, $Q^* = 0.0225 \text{ cm}^{-1}$ is expected.

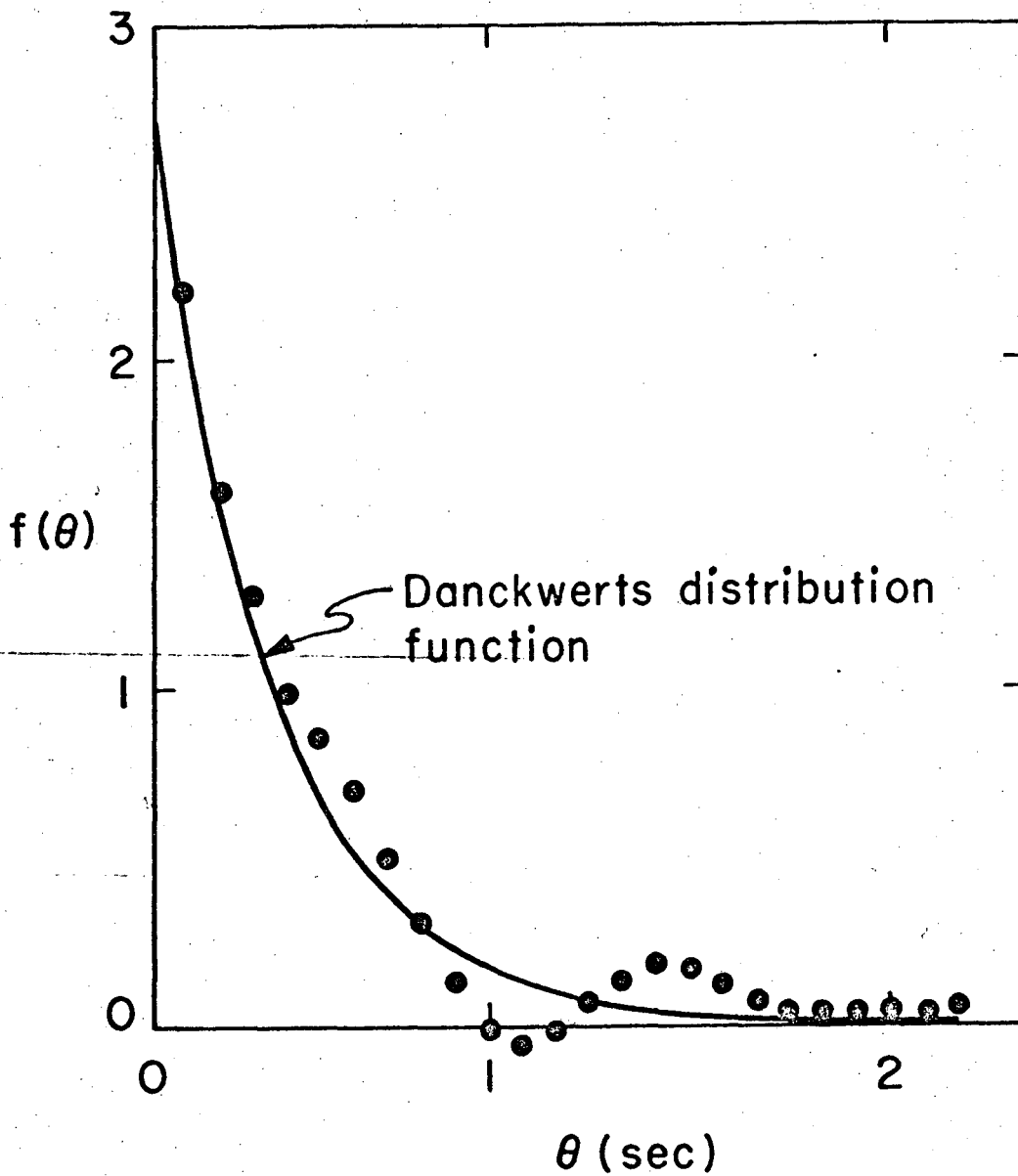
Application of Eq. (16) allows one to calculate the age distribution function of the interface; the result is shown in Fig. 4. The solid line in this figure represents the response predicted by a Danckwerts age distribution function based on values of s and Q^* from Table I.

A similar analysis of a turbulent, clean interface, obtained by stirring the liquid at a rate of 150 rpm is shown in Figs. 3 and 5. Table I shows the results of the least squares analysis as described by Eqs. (19) and (20).

Examination of these results indicates that under the conditions of these experiments the age distribution proposed by Danckwerts is a good approximation to that obtained experimentally. This means that under these conditions of turbulence the Danckwerts approximation may be used to predict mass transfer through the interface.

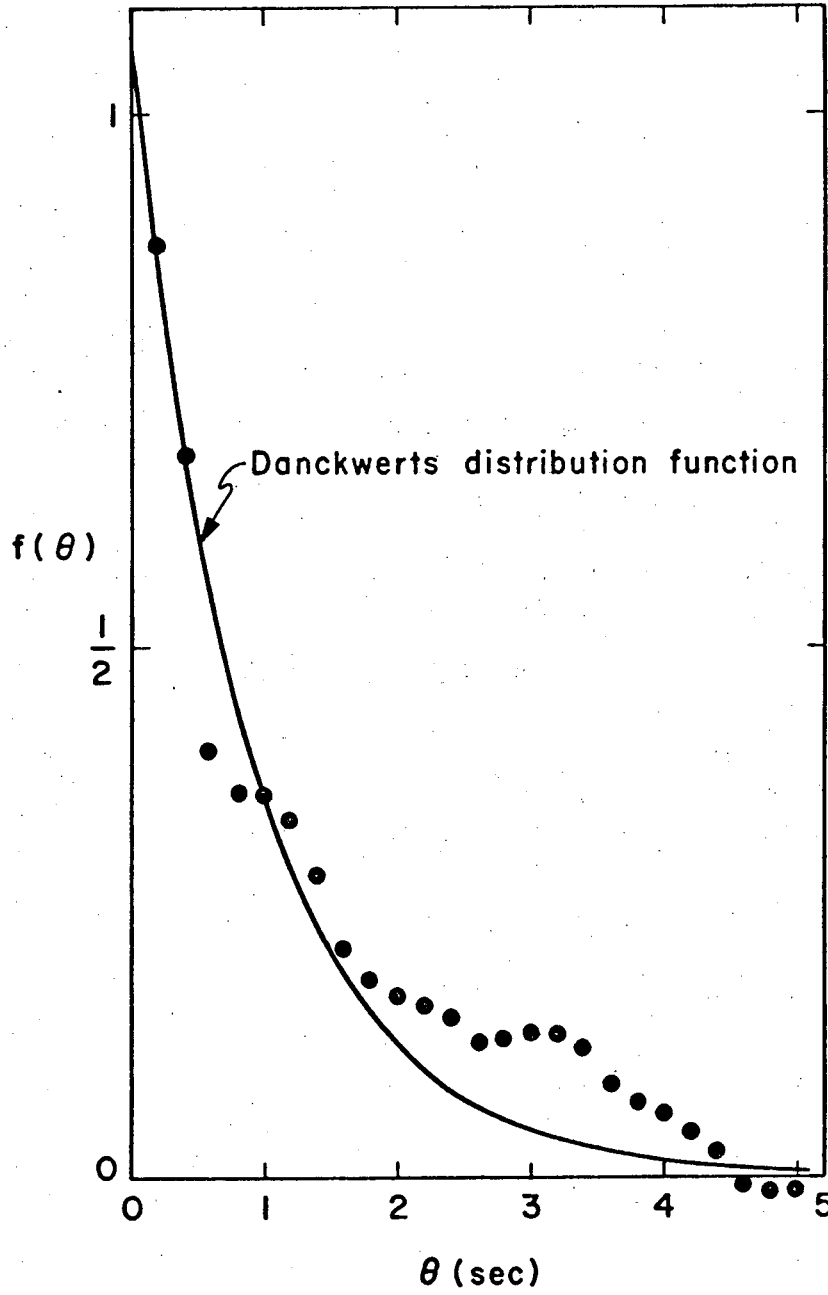
2. Effect of soluble Surfactants

A stagnant liquid of a specified concentration of the soluble surfactant sodium lauryl sulfonate was compared to an impermeable reference chamber. The frequency response revealed that no measurable change in mass transfer through the interface could be detected at all concentrations tested. The concentrations were 0.0001635-M,



XBL6910-3911

Fig. 4.



XBL6910-3917

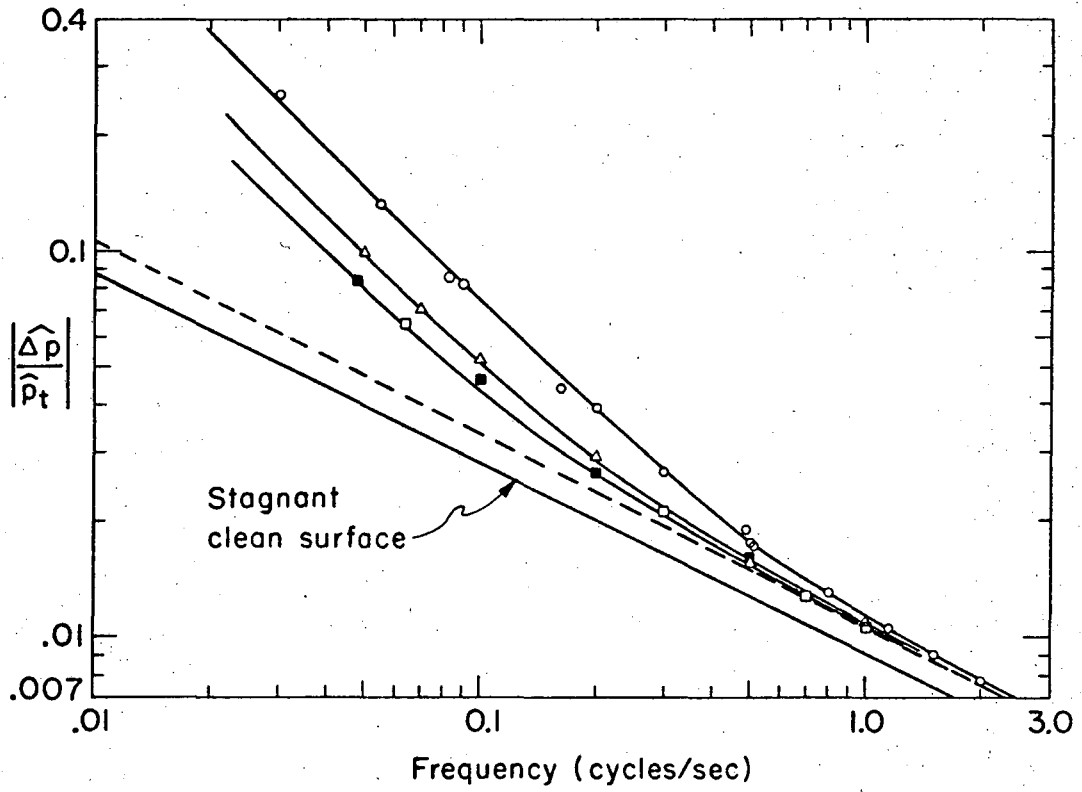
Fig. 5.

0.000327-M, and 0.00106-M. According to the Gibbs adsorption equation these concentrations correspond to surface excess concentrations approximately equivalent to 1/2, 1 and 3.1 monolayers, respectively, if one assumes that a surface concentration of approximately 10^{14} molecules/cm² is equivalent to a monolayer.

The effect of the soluble surfactant on transfer through a turbulent liquid interface was next examined. A turbulent interface, obtained by stirring the liquid at a rate of 230 rpm was compared with an impermeable surface. The frequency response results are shown in Fig. 6 for a clean, turbulent interface and for a turbulent liquid at the two lower concentrations of surfactant. The solid lines in the figure represent theoretical responses as explained earlier.

Tests were also carried out at a lower turbulence level, obtained by stirring the liquid at a rate of 150 rpm. The frequency response results were similar to those at the higher turbulence meaning that all concentrations tested showed the typical behavior shown in Fig. 6.

The turbulent data in the presence of sodium lauryl sulfonate were analyzed in the same manner as the clean interfaces. Calculation of the surface age distribution functions indicated that the surfactant did reduce the intensity of the turbulence at the given stirring speeds but did not affect the apparently random statistical nature of the surfaces. Thus, the assumptions of Danckwerts concerning random replacement of surface fluid elements are still very nearly true. The amplitude and phase data were treated separately according to Eqs. (19) and (20). The results are shown in Table II.



XBL6910-3914

Fig. 6.

Table II. Results of least squares analysis on data for water solutions of sodium lauryl sulfonate.

Stirring Speed rpm	Bulk Concentration moles/liter	Phase Data s, sec ⁻¹	Amplitude Data	
			s, sec ⁻¹	Q*, cm ⁻¹
150	0.0001635	0.864±0.192 ^a	0.853±0.106	0.0230±0.00006
150	0.000327	0.688±0.116	0.612±0.097	0.0235±0.00015
150	0.00106 ^b	0.578±0.180	0.507±0.034	0.0231±0.00004
230	0.0001635	1.29 ±0.07	1.22 ±0.250	0.0272±0.00024
230	0.000327	0.828±0.076	0.782±1.17	0.0274±0.00061
230	0.00106	0.699±0.060	2.42 ±0.66	0.026 ±0.001

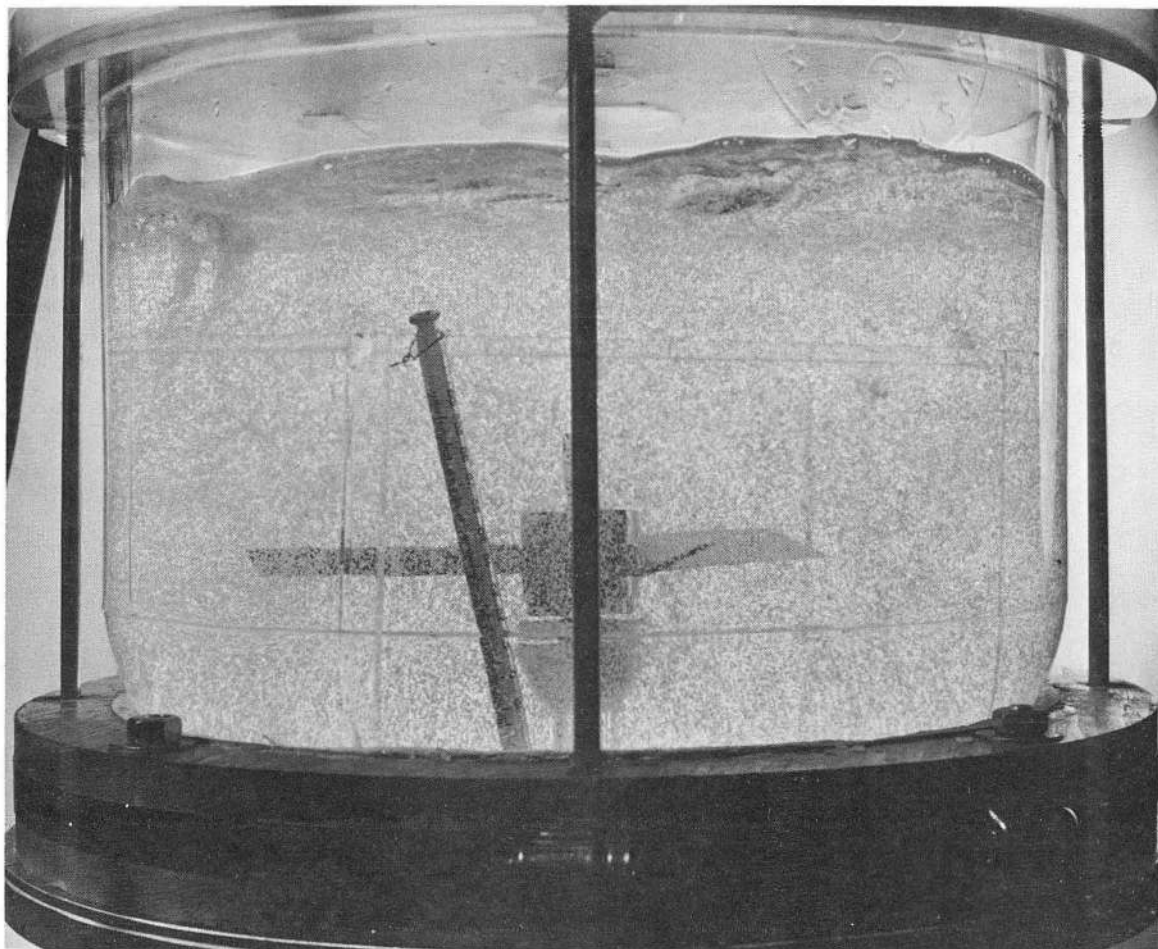
^aStandard error computed on the basis of 95% confidence level, i.e. approximately two standard deviations.

^bSodium lauryl sulfonate sample obtained from du Pont was used in this run only.

For the 0.00106-M liquid concentration of sodium lauryl sulfonate an unusual phenomena was observed at a stirring speed of 230 rpm. During pressure oscillations in the gas phase there occurred oscillating bubble nucleation and growth in the liquid phase. The nucleation and growth began as the gas pressure decreased and became a maximum when the gas pressure was smallest. As the gas pressure increased, the bubbles began to disappear and the bubble concentration was nearly zero at the maximum gas pressure. Figures 7 and 8 show the bubble concentrations at maximum and minimum values, respectively. These pictures were taken when the frequency of oscillation of the gas pressure was 0.1 cycles/sec. The formation and growth of bubbles was found nearly to disappear as the frequency increased to 0.7 cycles/sec.

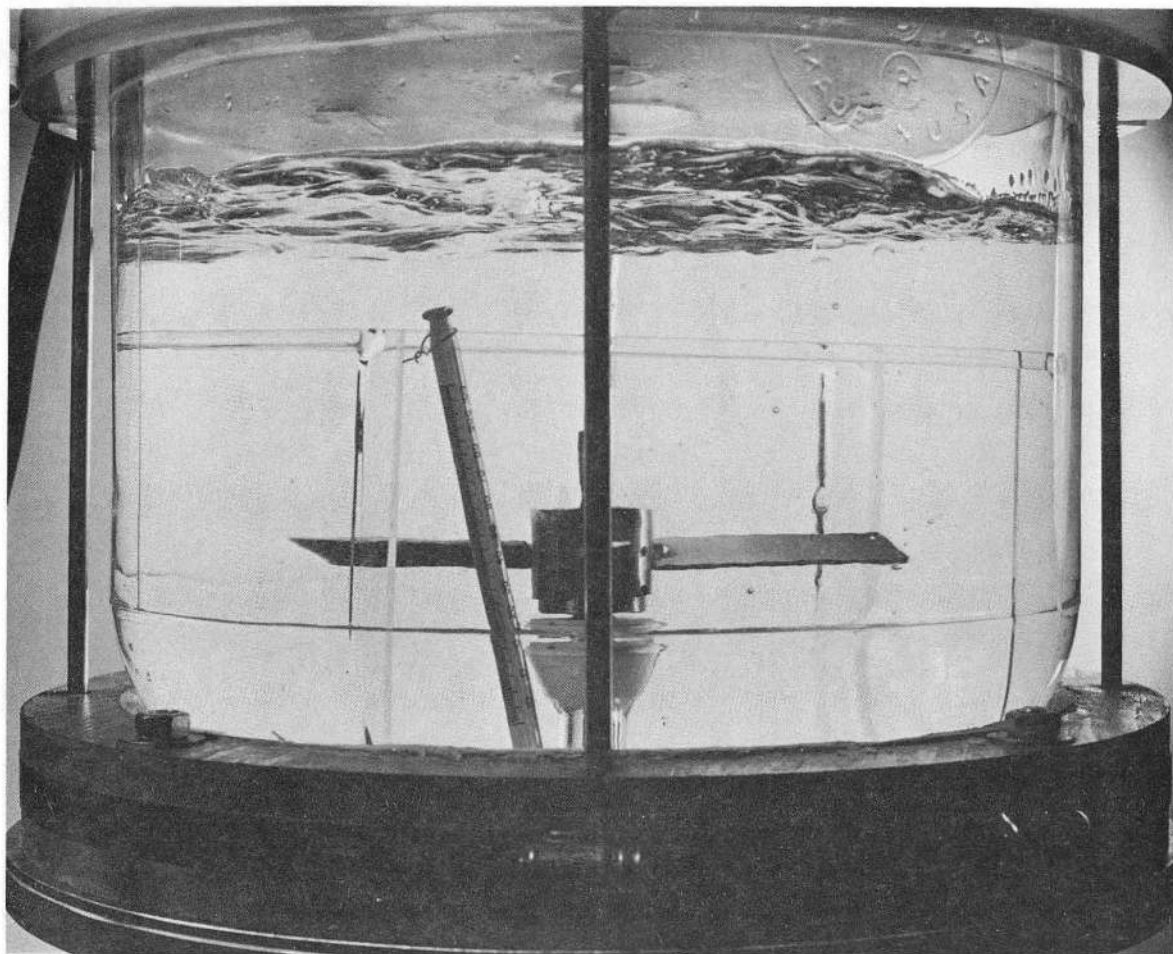
Treatment of the frequency response results according to the Danckwerts model showed a considerable difference between s values calculated from the amplitude and the phase data, as shown in Table II. Obviously, a Danckwerts distribution cannot reasonably describe these results. The oscillating bubble concentration caused the apparent liquid volume and the gas-liquid surface area to vary with time and also with frequency of oscillation. No reasonable conclusions could be drawn from these data.

The phenomenon apparently occurs because reduction of the gas pressure during oscillation produces a liquid solution that is slightly oversaturated. The reduction in surface tension owing to the surfactant's presence allows bubbles to form and grow more easily. At lower concentrations of surfactant very few bubbles were observed at any stirring



XBB 694-4064

Figure 7. Photograph of 0.00106-M sodium lauryl sulfonate solution at time of maximum bubble concentration. (stirring rate of 230 rpm)



XBB 694-4063

Figure 8. Photograph of 0.00106-M sodium lauryl sulfonate solution at time of minimum bubble concentration. (stirring rate, 230 rpm)

speed. Because of the intensity of stirring, a few entrained bubbles could be seen even in a pure liquid.

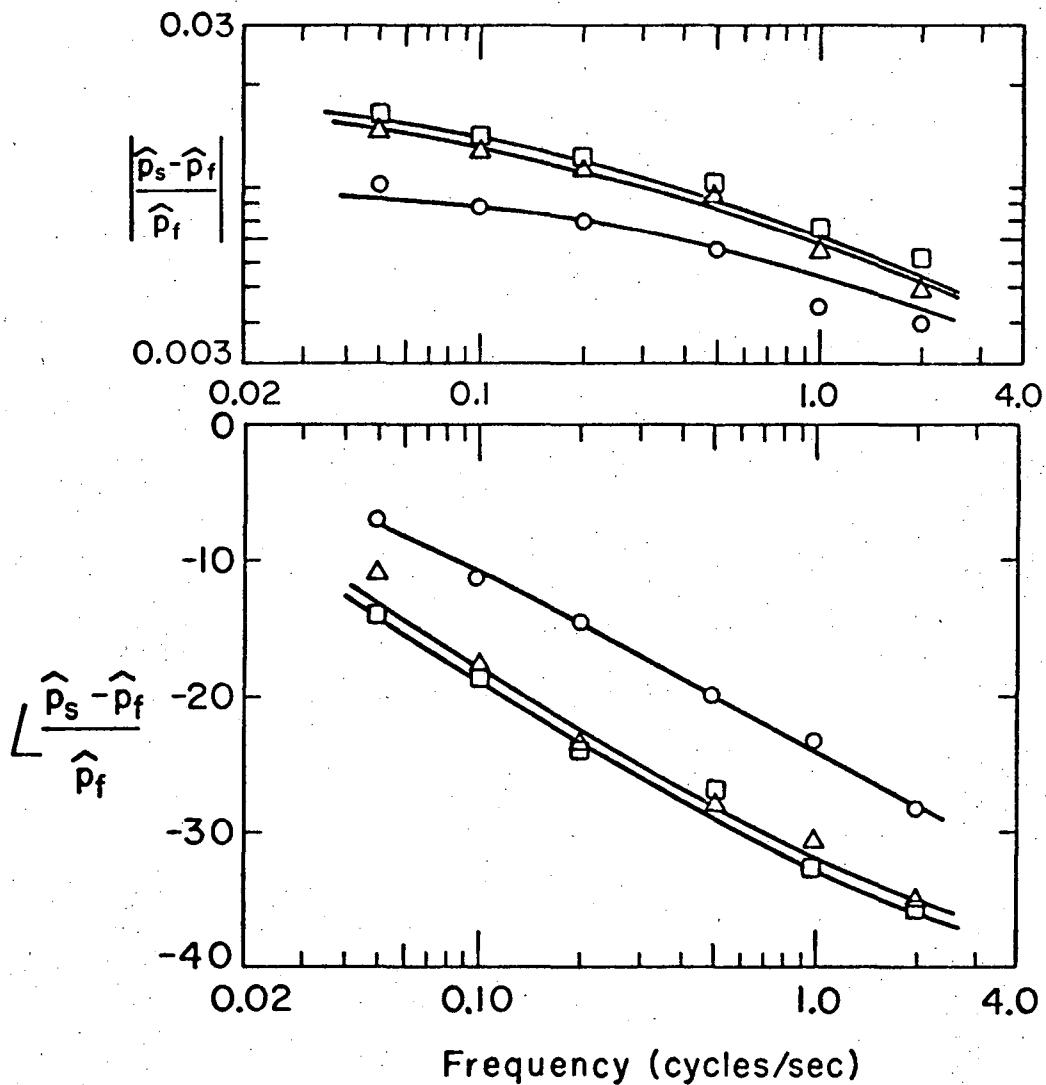
3. Effect of Insoluble Surfactants

Insoluble films of 1-hexadecanol were placed on the surface of a stationary liquid and compared to a clean stagnant liquid surface as a standard reference chamber. Concentrations equivalent to 1/2, 1 and 2 monolayers were tested. Unlike the results for a soluble film, a definite film resistance to gas transport was observed. Figure 9 shows the frequency response results for the three concentrations tested. The solid lines represent solutions to Eq. (21), using in each case the value of K_f which produced the best fit of the data (Table III).

The effect of the insoluble film on transfer through turbulent interfaces was next analyzed. Consider a turbulent surface covered with a film of 1-hexadecanol with the liquid stirred at a rate of 150 rpm. When this surface was compared to an impermeable surface as a standard reference, the results shown in Fig. 10 were obtained. The theoretical solid line in this figure corresponds to the results obtained for a clean turbulent interface. Concentrations equivalent to 1/2, 1 and 2 monolayers were used.

When the stirring rate was increased to 230 rpm similar results were obtained, indicating that insoluble films at these turbulence levels do not reduce mass transfer rates.

Results of the least squares analysis on the previous data according to a Danckwerts model are shown in Table IV.



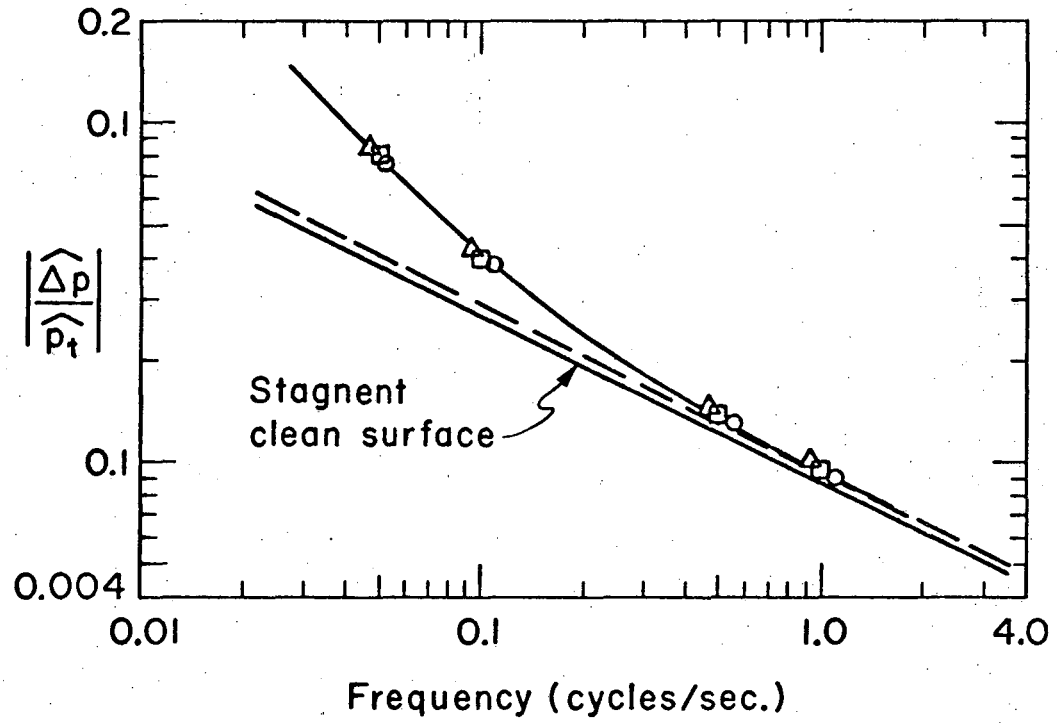
XBL6910-3919

Fig. 9.

Table III. Calculated film coefficients from least squares analysis of data for stagnant surfaces covered with 1-hexadecanol.

Surface Concentration in Equivalent Monolayers	Film Coefficient cm/sec
1/2	0.00754±0.00112
1	0.00385±0.00070
1 ^a	0.00446±0.00048
2	0.00364±0.00056

^aThese data were taken in a separate series of experiments by comparing a film-covered surface with an impermeable surface in the reference chamber.



XBL6910-3910

Fig. 10.

Table IV. Results of least squares analysis on turbulent data for 1-hexadecanol.

Stirring Speed rpm	Surface Concentration in Equivalent Monolayers	Phase Data	Amplitude Data	
		s, sec ⁻¹	s, sec ⁻¹	Q*, cm ⁻¹
150	1/2	1.16 ± 0.47 ^a	0.974 ± 0.175	0.0234 ± 0.00009
150	1	0.875 ± 0.226	1.01 ± 0.20	0.0231 ± 0.00011
150	2	0.914 ± 0.219	1.01 ± 0.21	0.0232 ± 0.00012
230	1/2	3.04 ± 0.31	2.29 ± 1.11	0.0280 ± 0.00149
230	1	3.16 ± 0.86	1.68 ± 1.53	0.0309 ± 0.00180
230	2	3.14 ± 1.51	1.51 ± 1.99	0.0311 ± 0.00214

^aStandard error computed on the basis of 95% confidence level, i.e. approximately two standard deviations.

DISCUSSION OF RESULTS

The results indicating that the soluble surfactant sodium lauryl sulfonate exhibits no measurable surface resistance is in accord with results of other researchers who investigated expanded-type surface layers (Bussey, 1966). Apparently the molecules in the surface are loosely bound and form an open lattice through which the gas molecules may easily pass. The measured resistance of a 1-hexadecanol film in the compressed state (i.e. at least 1 monolayer present) is compared with results of other researchers in Table V. Our measurements are in agreement with Plevan and Quinn (1966), who also used the sulfur dioxide-water system experimentally. An order of magnitude agreement is obtained between our work and others when the resistance of 1-hexadecanol films to passage of SO_2 molecules is compared with transport of CO_2 molecules. 1-hexadecanol molecules are believed to be closely packed together on the surface of water forming a rigid lattice through which gas molecules pass with some difficulty. By estimating the thickness of a monolayer film of 1-hexadecanol (approximately 25 Ångstroms) one may calculate the apparent diffusion coefficient of the gas molecules through the condensed monolayer. The result is on the order of 10^{-9} sq cm/sec. It seems that the surface film behaves more like a solid than a liquid.

The results of surfactant behavior at turbulent interfaces are more significant and qualitative explanation more difficult. In the presence of turbulence, several film properties come into play. A film must be able to withstand bombardment of the interface by eddies

Table V. The surface resistance of a 1-hexadecanol film compared with the results of previous investigations.

Source	Gas-Liquid System	Surface Resistance sec/cm
Blank <u>et al.</u> (1960)	CO ₂ -buffer	90 ^a
Sada <u>et al.</u> (1967)	CO ₂ -water	105
Plevan <u>et al.</u> (1966)	SO ₂ -water	170-215
This work	SO ₂ -water	224-275

^aAll resistances reported are for films with at least 1 monolayer equivalent surface concentration.

generated far from the surface. The elastic and flow properties of a film become important as the surface distorts owing to turbulence. If the scale of turbulence is large enough to cause the liquid surface to be broken, recovery of the film after collapse becomes important. The recovery speed may depend upon the adsorption rate at the interface, the surfactant's diffusion rate in the liquid, and perhaps even its diffusion rate across the surface. To attempt a reasonable explanation of the results obtained here, one needs to be able to estimate time constants for the above film phenomena. Let us briefly examine some of the properties of films reported in the literature.

A discussion of diffusion limited mass transfer rates of surfactants is given in Davies and Rideal (1961). They considered a system in which only a thin stagnant layer of liquid separated the surface film from the stirred bulk solution. The adsorption rate of surfactants was found from experiment to be strongly dependent on the surfactant's bulk concentration and was predicted well by an indicated theory. Application of this theory showed that for lauryl sulfate ions, after a sudden 10% change in surface concentration, the rate of adsorption was such that the surface was 60% restored to equilibrium after 6.4 milliseconds. The bulk concentration was 10^{-3} M. By contrast, consider lauryl alcohol at a surface concentration equivalent to approximately 1/2 monolayer. After a sudden 10% change in surface concentration, the rate of adsorption was such that the surface was 60% restored to equilibrium after 60 seconds. For derivatives with longer chains the rates become correspondingly smaller, and the times correspondingly longer.

Results of work by Hanson (1961) showed that adsorption was not solely diffusion limited. He stated, if it is assumed that spreading pressures depend on amounts of solute adsorbed and on subsurface concentration in the same manner in dynamic and equilibrium systems and if amounts of solute adsorbed and subsurface concentrations are inferred from observation of spreading pressure-time data on this basis, then adsorption limited solely by diffusion fails to explain the slow initial variation of spreading pressure with time. Except for this initial behavior, diffusion must play an important role in limiting the adsorption rate. The adsorption appears to be diffusion-controlled except for an initial time lag; times required to reach any particular spreading pressure are always longer than would be expected if diffusion alone were the limiting factor.

McArthur and Durham (1957) studied spreading rates of fatty alcohols that form condensed or rigid films. The time to spread a distance of 76 cm in a test chamber $91 \times 14 \times 10$ cm was measured. Spreading from 2 mm diameter particles of 85% cetyl alcohol required 15-18 minutes to reach a surface pressure of 20 dynes/cm. The equilibrium spreading pressure, or surface tension reduction, of cetyl alcohol is 44 dynes/cm. Recovery of spread films was assessed by compressing them until they collapsed and then observing the rate of increase of surface pressure. After spreading 95% cetyl alcohol, recovery to 20 dynes/cm requires 5 minutes.

Healy and La Mer (1964) studied damping of capillary waves by condensed monolayers and their effect on retardation of the evaporation

of water. Their experiments involved oscillation of a horizontal bar in a liquid surface at a given amplitude and frequency. They found that under dynamic conditions the surface pressure was reduced more than could be accounted for by the increase in surface area due to turbulence. They observed a maximum plateau for surface pressure under dynamic conditions much lower than the equilibrium spreading pressure, indicating that dynamic conditions may place a restriction on attainable surface pressure. They postulated that the reduction in surface pressure was due to submergence of monolayer molecules and concluded that the submergence should be highest at the bar. Nevertheless, no film breakage could be observed. They also found that recovery of the static surface pressure when the disturbance was removed was initially rapid but the final approach to equilibrium was slow.

Sakata and Berg (1969) measured the surface diffusivity of myristic acid, which forms an expanded surface layer. They found a surface diffusivity of 3×10^{-4} cm²/sec indicating that expanded monolayers behave much like a liquid. Blank and Britten (1965) predicted that the surface diffusivity of condensed layers, like 1-hexadecanol, should be on the order of 10^{-8} cm²/sec indicating a very rigid structure of the surface layer.

Application of the above information to interpretation of measured frequency responses at turbulent interfaces with surfactants present can be qualitative only. With the aid of this information, the following conclusions concerning surfactant behavior at turbulent interfaces seem reasonable.

The measured response of turbulent interfaces initially covered with 1-hexadecanol films indicates that the degree of turbulence was high enough that the rigid film must have been completely broken up and submerged in the bulk liquid. If one were to assume that the film was broken up into hydrocarbon particles on the order of 0.1 mm in diameter, Stokes Law would indicate that the time required to rise the average height of the bulk liquid (liquid depth is 8 inches) would be approximately 1.7 minutes. Since the spreading rate and the adsorption rate of 1-hexadecanol is very small compared to the average rate of submergence of any surface fluid element, it is unlikely that appreciable surfactant would be present on the stirred surface. The surfactant entering the surface through turbulent mixing will be immersed in a fluid element whose concentration will be equal to the very low bulk concentration of surfactant. Since only enough material was added to form a monolayer, mixing with the 10 liters of bulk liquid made the surfactant's concentration extremely small. Thus, only a small fraction of the surfactant originally added to the surface would exist there after the film is broken up. If one could reduce the turbulence low enough, there would be some level at which the monolayer would become stable. Under these conditions one could investigate possible damping of interfacial turbulence by condensed films. Unfortunately, in the experiments carried out here, the turbulence level could not be reduced much further without making the measured pressure-difference signal prohibitively small.

By comparing time for adsorption for the soluble surfactant with fluid element half lives, one can see that even if the film were broken some recovery should be obtained. As soon as a portion of the interface

is swept clean of surfactant, material immediately beneath can diffuse to the surface and adsorb. One can envision islands of surfactant on the turbulent surface. Fluid eddies which strike these areas from below may be slightly damped, as postulated by Davies (1964).

It must be reported that in all turbulent runs made that no visual change in the surface turbulence could be seen. Nevertheless, the measured average age of the surfaces ranged from approximately 0.3 - 2.0 seconds in experiments with and without surfactants.

These results indicate that owing to the nature of the surface films formed, a liquid type surface film can affect hydrodynamics at a turbulent interface even in the presence of vigorous turbulence, owing to the film's liquid mobility and fast rate of recovery. On the other hand, a condensed, insoluble film is very rigid and slow to recover after rupture. Its presence may only be important at low turbulence rates. The results reported by many researchers on the retardation of the rate of water evaporation help to strengthen this conclusion. They have found that even a slight wave action caused by wind or boating on water reservoirs considerably reduces the effectiveness of 1-hexadecanol films.

CONCLUSIONS

Although the interface impedance bridge is not simple to operate, it has yielded considerable information concerning interfacial turbulence. The apparatus is quite useful in measuring surface film resistances. It eliminates many problems encountered with previous techniques. Measurements can be carried out at small contact times, which were not possible previously, and density-driven convection currents have

negligible effect. The frequency response data allow one to examine the statistical nature of fluid interface as well as their time-average behavior.

The important problem of surfactant behavior at turbulent interfaces has been investigated. It was found that soluble films can dampen turbulence at the interface and reduce mass transfer rates, while insoluble films tend to break up and to have no measurable effect on mass transfer rates.

The results of this paper were drawn from data taken at high turbulence rates where the scale of turbulence was much greater than the depth of penetration of the dissolving gas. This type of turbulence is described well by the assumptions of Danckwerts (1951), as experimental results verify. As turbulence is reduced, these assumptions will no longer be valid and the relative motion of liquid at different levels close beneath the surface may not be disregarded. Solution of models of this type are much more difficult as can be seen in work by Scriven (1968) in which irrotational stagnation flow near interfaces is considered.

Another important problem not resolved here occurs when turbulence is not great enough to cause collapse of the condensed films. Surface resistance to gas transport plus possible hydrodynamic effects like those mentioned in the preceding paragraph may be present.

NOMENCLATURE

- A = area of liquid surface, sq cm
 c = concentration of gas in liquid, g-moles/liter
 D = diffusion coefficient of dissolved gas in liquid, sq cm/sec
 H = Henry's Law coefficient for gas in liquid, g-moles/(cc)(atm)
 k_L = liquid phase mass transfer coefficient, cm/sec
 K_f = surface film mass transfer coefficient, cm/sec
 n = number of moles of gas in chamber
 p = gas pressure, atm
 Q = $H A T_0 / V_0$
 Q^* = $Q D^{1/2}$
 R = gas constant, 82.06 (cc)(atm)/(g-mole)(°K)
 s = replacement frequency of fluid elements in liquid surface, sec⁻¹
 t = time, sec
 T_0 = temperature of surroundings, °K
 V = volume of gas space in chamber, cc
 x = distance from interface into liquid, cm
 ω = frequency, radians/sec

Subscripts:

- 0 = time-average value
 1 = chamber number, reference chamber
 2 = chamber number, test chamber
 f = film-covered surface
 t = turbulent surface

LITERATURE CITED

- Blank, M. and I. S. Britten, *J. Colloid Sci.*, 20, 789 (1965).
- Bussey, B. W., Ph.D. Thesis in Chemical Engineering, University of Delaware, (1966).
- Danckwerts, P. V., *Ind. Eng. Chem.*, 43, 1460 (1951).
- Davies, J. T., "The Effects of Surface Films in Damping Eddies at a Free Surface of a Turbulent Liquid," paper presented at Boston meeting of the A. I. Ch. E. in December, 1964.
- Davies, J. T. and E. K. Rideal, Interfacial Phenomena (Academic Press, New York, 1961).
- Erdelyi, A., Ed., Table of Integral Transforms (McGraw-Hill, New York, 1954), Vol. I.
- Gaines, G. L., Insoluble Monolayers at Liquid-Gas Interfaces (Interscience Publishers, New York, 1966).
- Hanson, R. S., *J. Colloid Sci.*, 16, 549 (1961).
- Hanson, R. S. and J. Lucassen, *J. Colloid Interface Sci.*, 22, 32 (1966).
- Healy, T. W. and V. K. La Mer, *J. Phys. Chem.*, 68, 3535 (1964).
- Lamb, W. B., Ph.D. Thesis in Engineering, University of Delaware, (1965).
- McArthur, I. K. H. and K. Durham, in Proceedings of the Second International Congress of Surface Activity, (Academic Press, New York, 1957), Vol. 1, p. 262.
- Plevan, R. E. and J. A. Quinn, *A. I. Ch. E. J.*, 12, 894 (1964).
- Posner, A. M. and A. E. Alexander, *Trans. Faraday Soc.*, 45, 651 (1949).
- Ries, H. E. and W. A. Kimball, in Proceedings of the Second International Congress of Surface Activity, (Academic Press, New York, 1957), Vol. 1, p. 75.

Sada, E. and D. M. Himmelblau, A. I. Ch. E. J., 13, 860 (1967).

Sakata, E. K. and J. C. Berg, Ind. Eng. Chem., Fundamentals, 8, 570
(1969).

Scriven, L. E., Chem. Eng. Educ., 2, 145 (1969).

Springer, T. G., Ph.D. Thesis in Chemical Engineering, University of
California, Berkeley, (1969).

Whitaker, S. L. and R. L. Pigford, A. I. Ch. E. J., 12, 741 (1966).

LIST OF FIGURES

- Fig. 1. Surface tension of sodium lauryl sulfonate versus bulk liquid concentration.
- Fig. 2. Surface tension of 1-hexadecanol films versus equivalent surface concentration in monolayers.
- Fig. 3. Bridge comparison of a clean, turbulent water interface with an impermeable surface. (○ -liquid stirred at a rate of 230 rpm; □ -liquid stirred at a rate of 150 rpm.)
- Fig. 4. Surface age distribution function versus surface element age for a liquid stirred at a rate of 230 rpm. Data points obtained with Eq. (16).
- Fig. 5. Surface age distribution function versus surface element age for a liquid stirred at a rate of 150 rpm. Data points obtained with Eq. (16).
- Fig. 6. Bridge comparison of turbulent sodium lauryl sulfonate solutions (stirring rate of 230 rpm) with an impermeable surface. (○ -clean liquid; Δ -0.0001635-M solution; □ -0.000327-M solution.)
- Fig. 7. Photograph of 0.00106-M sodium lauryl sulfonate solution at time of maximum bubble concentration, (stirring rate of 230 rpm).
- Fig. 8. Photograph of 0.00106-M sodium lauryl sulfonate solution at time of minimum bubble concentration, (stirring rate, 230 rpm).
- Fig. 9. Bridge comparison of a stagnant liquid surface, covered by a 1-hexadecanol film, with a clean, stagnant liquid surface. (○ -1/2 monolayer equivalent surface concentration; Δ -1 monolayer; □ -2 monolayers).

Fig. 10. Bridge comparison of a turbulent interface (stirring speed, 150 rpm), 1-hexadecanol surface film added, with an impermeable surface. (○ -1/2 monolayer equivalent surface concentration; Δ -1 monolayer; □ -2 monolayers.)

Tabulation of Individual Runs

Run Number	Signal Measured	Interface Conditions
1-8	$(p_s - p_t)/p_t$	Clean, Turbulent-230 rpm
9	$(p_f - p_s)/p_f$	Stagnant, 0.000327-M sodium lauryl sulfonate
10	$(p_s - p_t)/p_t$	Turbulent-230 rpm, 0.000327-M sodium lauryl sulfonate
11	$(p_I - p_t)/p_t$	Turbulent-230 rpm, 0.000327-M sodium lauryl sulfonate
12	$(p_s - p_t)/p_t$	Turbulent-150 rpm, 0.000327-M sodium lauryl sulfonate
13	$(p_f - p_s)/p_f$	Stagnant, 0.00106-M sodium lauryl sulfonate
14	$(p_I - p_t)/p_t$	Turbulent-230 rpm, 0.00106-M sodium lauryl sulfonate
15	$(p_s - p_t)/p_t$	Turbulent-230 rpm, 0.00106-M sodium lauryl sulfonate
16	$(p_I - p_t)/p_t$	Clean, Turbulent-150 rpm
17	$(p_s - p_t)/p_t$	Clean, Turbulent-150 rpm
18-20	$(p_I - p_f)/p_t$	Stagnant, 1 monolayer 1-hexadecanol
21-26	$(p_f - p_s)/p_f$	Stagnant, 1/2, 1 & 2 monolayer 1-hexadecanol
27-30	$(p_s - p_t)/p_t$	Turbulent-150 & 230 rpm 1/2, 1 & 2 monolayer 1-hexadecanol
31-32	$(p_I - p_s)/p_s$	Clean, Stagnant
33-34	$(p_s - p_t)/p_t$	Turbulent-150 & 230 rpm 0.0001635-M sodium lauryl sulfonate

(continued)

Tabulation of Individual Runs Continued

Run Number	Signal Measured	Interface Conditions
36	$(p_s - p_t)/p_t$	Turbulent-150 rpm, 0.00106-M sodium lauryl sulfonate

Run # 1-8

Type of Reference Chamber (Chamber 1)	Clean, Stagnant Surface
Surface Conditions of Test Chamber (Chamber 2)	Turbulent, 230 rpm stirring speed
Surfactant	None

	<u>Reference Chamber</u>	<u>Test Chamber</u>
Liquid Temp. (°C)	25.5-26.0	25.5-26.0
Gas Space Height (cm)	3.175-3.227	2.859-2.870

Frequency cycles/sec	Comparison of Stagnant and Turbulent Surface (Measured Signal)		Comparison of Impermeable and Turbulent Interface (Calculated Signal)	
		$(\hat{p}_1 - \hat{p}_2)/\hat{p}_2$		$(\hat{p}_I - \hat{p}_t)/\hat{p}_t$
0.03	0.212	∠ -95.6	0.255	∠ -88.6
0.055	0.104	∠ -99.1	0.132	∠ -87.0
0.083	0.0635	∠ -101.9	0.0855	∠ -85.4
0.090	0.0609	∠ -101.9	0.0820	∠ -85.3
0.167	0.0286	∠ -104.6	0.0442	∠ -80.1
0.20	0.0247	∠ -104.7	0.0390	∠ -79.1
0.30	0.0146	∠ -105.7	0.0268	∠ -74.2
0.48	0.00858	∠ -102.3	0.0190	∠ -67.8
0.50	0.00712	∠ -103.5	0.0175	∠ -65.8
0.51	0.00693	∠ -102.9	0.0173	∠ -65.3
0.80	0.00418	∠ -96.7	0.0130	∠ -59.9
1.15	0.00277	∠ -90.0	0.0105	∠ -55.9
1.50	0.00202	∠ -83.5	0.00900	∠ -53.2
2.00	0.00162	∠ -77.7	0.00777	∠ -51.6

Run # 9

Type of Reference Chamber (Chamber 1)	Clean, Stagnant Surface
Surface Conditions of Test Chamber (Chamber 2)	Stagnant
Surfactant	0.000327-M sodium lauryl sulfonate

	<u>Reference Chamber</u>	<u>Test Chamber</u>
Liquid Temp. (°C)	25.9	26.5
Gas Space Height (cm)	3.37	2.82

Frequency cycles/sec	Comparison of Two Stagnant Surfaces (Balance Signal) $ (p_1 - p_2)/p_2 $	Comparison of a Stagnant and Film-Covered Stagnant Surface (Measured Signal) $ (p_s - p_f)/p_f $
0.07	0.00033	0.00064
0.10	0.0005	0.00073
0.30	0.00087	0.00073
0.50	0.00118	0.0011
1.00	0.00105	0.0012

Run # 10

Type of Reference Chamber (Chamber 1)	Clean, Stagnant Surface
Surface Conditions of Test Chamber (Chamber 2)	Turbulent-230 rpm stirring speed
Surfactant	0.000327-M sodium lauryl sulfonate

	<u>Reference Chamber</u>	<u>Test Chamber</u>
Liquid Temp. (°C)	25.9	26.5
Gas Space Height (cm)	3.212	2.820

Frequency cycles/sec	Comparison of Stagnant and Turbulent Surface (Measured Signal)		Comparison of Impermeable and Turbulent Interface (Calculated Signal)	
		$(\hat{p}_1 - \hat{p}_2)/\hat{p}_2$		$(\hat{p}_I - \hat{p}_t)/\hat{p}_t$
0.064	0.0381	∠ -102.8	0.0648	∠ -76.4
0.30	0.00561	∠ -85.0	0.021	∠ -55.2
0.70	0.00232	∠ -74.9	0.0128	∠ -50.4
1.00	0.00191	∠ -64.9	0.0108	∠ -48.6

Run # 11

Type of Reference Chamber (Chamber 1)	Impermeable Surface
Surface Conditions of Test Chamber (Chamber 2)	Turbulent, 230 rpm stirring speed
Surfactant	0.000327-M sodium lauryl sulfonate

	<u>Reference Chamber</u>	<u>Test Chamber</u>
Liquid Temp. (°C)	25.9	26.5
Gas Space Height (cm)	3.212	2.82

Frequency cycles/sec	Comparison of Impermeable and Turbulent Interface (Measured Signal)		Comparison of Stagnant and Turbulent Interface (Calculated Signal)	
		$(\hat{p}_1 - \hat{p}_2)/\hat{p}_2$		$(\hat{p}_s - \hat{p}_t)/\hat{p}_t$
0.048	0.0830	L -80.0	0.0531	L -103.5
0.10	0.0459	L -72.0	0.0238	L -102.6
0.20	0.0266	L -60.0	0.00873	L -94.6
0.50	0.016	L -53.1	0.00382	L -79.9
1.00	0.0112	L -48.8	0.00230	L -63.0

Run # 12

Type of Reference Chamber (Chamber 1)	Clean, Stagnant Surface
Surface Conditions of Test Chamber (Chamber 2)	Turbulent, 150 rpm stirring speed
Surfactant	0.000327-M sodium lauryl sulfonate

	<u>Reference Chamber</u>	<u>Test Chamber</u>
Liquid Temp. (°C)	25.8	26.2
Gas Space Height (cm)	3.175	2.86

Frequency cycles/sec	Comparison of Stagnant and Turbulent Surface (Measured Signal)		Comparison of Impermeable and Turbulent Interface Calculated Signal)	
		$(\hat{p}_1 - \hat{p}_2)/\hat{p}_2$		$(\hat{p}_I - \hat{p}_t)/\hat{p}_t$
0.05	0.0336	∠ -112.0	0.0618	∠ -76.6
0.07	0.0242	∠ -114.3	0.0482	∠ -74.2
0.10	0.0144	∠ -116.6	0.0356	∠ -68.4
0.20	0.00491	∠ -120.3	0.0218	∠ -57.9
0.30	0.00304	∠ -118.3	0.0175	∠ -54.9
0.50	0.00153	∠ -110.6	0.0134	∠ -51.2

Run # 13

Type of Reference Chamber (Chamber 1)	Clean, Stagnant Surface
Surface Conditions of Test Chamber (Chamber 2)	Stagnant
Surfactant	0.00106-M sodium lauryl sulfonate

	<u>Reference Chamber</u>	<u>Test Chamber</u>
Liquid Temp. (°C)	26.0	26.3
Gas Space Height (cm)	3.175	2.86

Frequency cycles/sec	Comparison of two Stagnant Surfaces (Balance Signal) $ (p_1 - p_2)/p_2 $	Comparison of Stagnant and Film-Covered Stagnant Surface (Measured Signal) $ (p_s - p_f)/p_f $
0.10	0.00005	0.00018
0.30	0.00073	0.00046
0.50	0.00185	0.0017
1.00	0.00087	0.00087

Run # 14

Type of Reference Chamber (Chamber 1)	Impermeable Surface
Surface Conditions of Test Chamber (Chamber 2)	Turbulent, 230 rpm stirring speed
Surfactant	0.00106-M sodium lauryl sulfonate

	<u>Reference Chamber</u>	<u>Test Chamber</u>
Liquid Temp. (°C)	26.2	26.5
Gas Space Height (cm)	2.937	2.86

Frequency cycles/sec	Comparison of Impermeable and Turbulent Interface (Measured Signal)		Comparison of Stagnant and Turbulent Interface (Calculated Signal)	
		$(\hat{p}_1 - \hat{p}_2)/\hat{p}_2$		$(\hat{p}_s - \hat{p}_t)/\hat{p}_t$
0.05	0.113	∠ -77.5	0.0797	∠ -90.2
0.10	0.063	∠ -71.0	0.0387	∠ -88.2
0.20	0.0324	∠ -60.0	0.0138	∠ -80.9
0.50	0.0166	∠ -51.5	0.00419	∠ -70.6

Run # 15

Type of Reference Chamber (Chamber 1)	Clean, Stagnant Surface
Surface Conditions of Test Chamber (Chamber 2)	Turbulent, 230 rpm stirring speed
Surfactant	0.00106-M sodium lauryl sulfonate

	<u>Reference Chamber</u>	<u>Test Chamber</u>
Liquid Temp. (°C)	26.1	26.4
Gas Space Height (cm)	3.21	2.86

Frequency cycles/sec	Comparison of Stagnant and Turbulent Surface (Measured Signal)		Comparison of Impermeable and Turbulent Interface (Calculated Signal)	
	$(\hat{p}_1 - \hat{p}_2)/\hat{p}_2$		$(\hat{p}_I - \hat{p}_t)/\hat{p}_t$	
0.30	0.0100	∠ -71.4	0.0258	∠ -55.3
0.50	0.00468	∠ -67.0	0.0172	∠ -51.1
1.00	0.00179	∠ -63.6	0.0107	∠ -48.2

Run # 16

Type of Reference Chamber (Chamber 1)	Impermeable Surface
Surface Conditions of Test Chamber (Chamber 2)	Turbulent, 150 rpm stirring speed
Surfactant	None

	<u>Reference Chamber</u>	<u>Test Chamber</u>
Liquid Temp. (°C)	25.9	26.2
Gas Space Height (cm)	3.33	2.86

Frequency cycles/sec	Comparison of Impermeable and Turbulent Interface (Measured Signal)		Comparison of Stagnant and Turbulent Interface (Calculated Signal)	
		$(\hat{p}_1 - \hat{p}_2)/\hat{p}_2$		$(\hat{p}_s - \hat{p}_t)/\hat{p}_t$
0.05	0.0785	∠ -81.50	0.0505	∠ -107.0
0.07	0.0548	∠ -79.4	0.0321	∠ -113.3
0.10	0.0414	∠ -75.0	0.0215	∠ -113.7
0.20	0.0240	∠ -64.6	0.00828	∠ -116.4
0.30	0.0185	∠ -59.6	0.00482	∠ -116.0

Run # 17

Type of Reference Chamber (Chamber 1)	Clean, Stagnant Surface
Surface Conditions of Test Chamber (Chamber 2)	Turbulent, 150 rpm stirring speed
Surfactant	None

	<u>Reference Chamber</u>	<u>Test Chamber</u>
Liquid Temp. (°C)	25.9	26.2
Gas Space Height (cm)	3.33	2.86

Frequency cycles/sec	Comparison of Stagnant and Turbulent Surface (Measured Signal)		Comparison of Impermeable and Turbulent Interface (Calculated Signal)	
	$(\hat{p}_1 - \hat{p}_2)/\hat{p}_2$		$(\hat{p}_I - \hat{p}_t)/\hat{p}_t$	
0.10	0.0211	∠ -113.4	0.0412	∠ -74.5
0.50	0.00234	∠ -116.6	0.0136	∠ -54.6
1.00	0.00083	∠ -108.4	0.00937	∠ -49.7

Run # 18-20

Type of Reference Chamber (Chamber 1)	Impermeable Surface
Surface Conditions of Test Chamber (Chamber 2)	Stagnant
Surfactant	1-monolayer of 1-hexadecanol

	<u>Reference Chamber</u>	<u>Test Chamber</u>
Liquid Temp. (°C)	25.9	26.0
Gas Space Height (cm)	3.175	2.86

Frequency cycles/sec	Comparison of Impermeable and Film-Covered Stagnant Surface (Measured Signal)		Comparison of a Stagnant and Film-Covered Stagnant Surface (Calculated Signal)	
		$(\hat{p}_1 - \hat{p}_2)/\hat{p}_2$		$(\hat{p}_f - \hat{p}_s)/\hat{p}_f$
0.05	0.0300	∠ -58.0	0.0124	∠ -11.9
0.10	0.0167	∠ -62.3	0.0131	∠ -22.3
0.20	0.0110	∠ -67.3	0.0106	∠ -21.5
0.50	0.00560	∠ -73.0	0.00810	∠ -25.9
1.00	0.00286	∠ -76.7	0.00667	∠ -31.8
2.00	0.00180	∠ -75.7	0.00486	∠ -34.0

Run # 21-26

Type of Reference Chamber (Chamber 1)	Clean, Stagnant Surface
Surface Conditions of Test Chamber (Chamber 2)	Stagnant
Surfactant	1/2-monolayer of 1-hexadecanol

	<u>Reference Chamber</u>	<u>Test Chamber</u>
Liquid Temp. (°C)	23.4	23.8
Gas Space Height (cm)	3.175	2.86

Frequency cycles/sec	Comparison of a Stagnant and Film-Covered Stagnant Surface (Measured Signal)		Comparison of Impermeable and Film-Covered Stagnant Surface (Calculated Signal)	
	$(\hat{p}_2 - \hat{p}_1)/\hat{p}_1$		$(\hat{p}_I - \hat{p}_f)/\hat{p}_f$	
0.05	0.0100	∠ -7.0	0.0324	∠ -56.0
0.10	0.00850	∠ -11.7	0.0216	∠ -57.5
0.20	0.00784	∠ -14.8	0.0137	∠ -61.7
0.50	0.00648	∠ -20.2	0.00726	∠ -67.0
1.00	0.00431	∠ -23.9	0.00516	∠ -62.5
2.00	0.00383	∠ -29.1	0.00284	∠ -66.6

Run # 21-26

Type of Reference Chamber (Chamber 1)	Clean, Stagnant Surface
Surface Conditions of Test Chamber (Chamber 2)	Stagnant
Surfactant	1 monolayer of 1-hexadecanol

	<u>Reference Chamber</u>	<u>Test Chamber</u>
Liquid Temp. (°C)	23.4	23.8
Gas Space Height (cm)	3.175	2.86

Frequency cycles/sec	Comparison of a Stagnant and Film-Covered Stagnant Surface (Measured Signal)		Comparison of Impermeable and Film-Covered Stagnant Surface (Calculated Signal)	
		$(\hat{p}_2 - \hat{p}_1)/\hat{p}_1$		$(\hat{p}_I - \hat{p}_f)/\hat{p}_f$
0.05	0.0142	∠ -11.0	0.0289	∠ -60.8
0.10	0.0124	∠ -17.9	0.0179	∠ -63.2
0.20	0.0112	∠ -23.5	0.0103	∠ -68.1
0.50	0.00925	∠ -28.1	0.00458	∠ -80.3
1.00	0.00643	∠ -30.9	0.00310	∠ -75.0
2.00	0.00490	∠ -35.5	0.00169	∠ -73.3

Run # 21-26

Type of Reference Chamber (Chamber 1)	Clean, Stagnant Surface
Surface Conditions of Test Chamber (Chamber 2)	Stagnant
Surfactant	2 monolayers of 1-hexadecanol

	<u>Reference Chamber</u>	<u>Test Chamber</u>
Liquid Temp. (°C)	23.4	23.8
Gas Space Height (cm)	3.175	2.86

Frequency cycles/sec	Comparison of a Stagnant and Film-Covered Surface (Measured Signal)		Comparison of Impermeable and Film-Covered Stagnant Surface (Calculated Signal)	
	$(\hat{p}_2 - \hat{p}_1)/\hat{p}_1$		$(\hat{p}_I - \hat{p}_f)/\hat{p}_f$	
0.05	0.0160	∠ -14.2	0.0270	∠ -62.5
0.10	0.0135	∠ -18.3	0.0170	∠ -65.5
0.20	0.0122	∠ -24.0	0.00949	∠ -71.9
0.50	0.00942	∠ -27.6	0.00454	∠ -82.8
1.00	0.00731	∠ -32.9	0.00233	∠ -85.5
2.00	0.00591	∠ -35.7	0.00106	∠ -107.7

Run # 27

Frequency = 1.00 cycles/sec for all data shown below

Type of Reference Chamber (Chamber 1) Clean, Stagnant Surface

Surfactant 1-hexadecanol

	Reference Chamber	Test Chamber
Liquid Temp. (°C)	23.5	24.0
Gas Space Height (cm)	3.175	2.86

Surface Conditions	Comparison of Stagnant and Indicated Surface (Measured Signal)		Comparison of Impermeable and Indicated Surface (Calculated Signal)	
		$(\hat{p}_1 - \hat{p}_2)/\hat{p}_2$		$(\hat{p}_1 - \hat{p})/\hat{p}$
stagnant, 0.5 ^a	0.00565	∠ -25.6	0.00406	∠ -72.4
turbulent-150 ^b , 0.5	0.00090	∠ -110.8	0.00938	∠ -50.2
stagnant, 0.5	0.00511	∠ -25.5	0.00445	∠ -67.4
turbulent-230, 0.5	0.00344	∠ -92.3	0.0116	∠ -58.0
stagnant, 0.5	0.00432	∠ -25.7	0.00506	∠ -61.3
stagnant, 1.0	0.00696	∠ -32.9	0.00256	∠ -79.1
turbulent-150, 1.0	0.00068	∠ -110.1	0.00928	∠ -49.0
stagnant, 1.0	0.00698	∠ -31.5	0.00273	∠ -80.1
turbulent-230, 1.0	0.00438	∠ -86.7	0.0126	∠ -58.6
stagnant, 1.0	0.00671	∠ -32.8	0.00275	∠ -75.7
stagnant, 2.0	0.00783	∠ -32.9	0.00205	∠ -96.8
turbulent-150, 2.0	0.00072	∠ -109.6	0.00930	∠ -49.1
stagnant, 2.0	0.00675	∠ -31.7	0.00281	∠ -78.1
turbulent-230, 2.0	0.00440	∠ -85.5	0.0127	∠ -58.3

^aSurface concentration of 1-hexadecanol in equivalent monolayers.

^bStirring speed producing the turbulence in rev/min.

Run # 28

 Frequency = 0.50 cycles/sec for all data shown below

Type of Reference Chamber (Chamber 1) Clean, Stagnant Surface

Surfactant 1-hexadecanol

	<u>Reference Chamber</u>	<u>Test Chamber</u>
Liquid Temp. (°C)	23.5	24.0
Gas Space Height (cm)	3.21	2.86

Surface Conditions	Comparison of Stagnant and Indicated Surface (Measured Signal)		Comparison of Impermeable and Indicated Surface (Calculated Signal)	
		$(\hat{p}_1 - \hat{p}_2)\hat{p}_2$		$(\hat{p}_I - \hat{p})/\hat{p}$
stagnant, 0.5 ^a	0.00689	∠ -20.7	0.00693	∠ -69.0
turbulent-150 ^b , 0.5	0.00208	∠ -118.4	0.0134	∠ -53.8
stagnant, 0.5	0.00649	∠ -19.6	0.00730	∠ -67.4
turbulent-230, 0.5	0.00644	∠ -102.6	0.0170	∠ -64.0
stagnant, 0.5	0.00570	∠ -18.4	0.00795	∠ -63.7
stagnant, 1.0	0.00817	∠ -28.9	0.00525	∠ -70.1
turbulent-150, 1.0	0.00210	∠ -120.6	0.0134	∠ -53.9
stagnant, 1.0	0.00787	∠ -27.9	0.00557	∠ -69.2
turbulent-230, 1.0	0.00704	∠ -102.6	0.0175	∠ -65.3
stagnant, 1.0	0.00657	∠ -27.6	0.00664	∠ -62.0
stagnant, 2.0	0.00917	∠ -30.0	0.00440	∠ -76.9
turbulent-150, 2.0	0.00218	∠ -120.5	0.0134	∠ -54.2
stagnant, 2.0	0.00817	∠ -28.9	0.00525	∠ -70.1
turbulent-230, 2.0	0.00654	∠ -102.6	0.0171	∠ -64.2

^a Surface concentration of 1-hexadecanol in equivalent monolayers.

^b Stirring speed producing the turbulence in rev/min.

Run # 29

Frequency = 0.10 cycles/sec for all data shown below

Type of Reference Chamber Clean, Stagnant Surface
(Chamber 1)

Surfactant 1-hexadecanol

	<u>Reference Chamber</u>	<u>Test Chamber</u>
Liquid Temp. (°C)	23.5	24.0
Gas Space Height (cm)	3.135	2.86

Surface Conditions	Comparison of Stagnant and Indicated Surface (Measured Signal)		Comparison of Impermeable and Indicated Surface (Calculated Signal)	
	$(\hat{p}_1 - \hat{p}_2)/\hat{p}_2$		$(\hat{p}_I - \hat{p})/\hat{p}$	
stagnant, 0.5 ^a	0.00804	∠ -12.6	0.0218	∠ -56.4
turbulent-150 ^b , 0.5	0.0203	∠ -114.3	0.0403	∠ -74.1
stagnant, 0.5	0.00734	∠ -13.3	0.0223	∠ -55.0
turbulent-230, 0.5	0.0543	∠ -100.6	0.0748	∠ -83.5
stagnant, 0.5	0.00710	∠ -16.2	0.0222	∠ -53.8
stagnant, 1.0	0.0132	∠ -21.4	0.0168	∠ -63.0
turbulent-150, 1.0	0.0188	∠ -116.4	0.0387	∠ -73.4
stagnant, 1.0	0.0113	∠ -22.3	0.0182	∠ -58.6
turbulent-230, 1.0	0.0544	∠ -104.1	0.0738	∠ -85.9
stagnant, 1.0	0.0113	∠ -22.4	0.0182	∠ -58.6
stagnant, 2.0	0.0143	∠ -20.9	0.0160	∠ -65.9
turbulent-150, 2.0	0.0189	∠ -116.4	0.0388	∠ -73.5
stagnant, 2.0	0.0140	∠ -21.0	0.0162	∠ -65.1
turbulent-230, 2.0	0.0523	∠ -100.7	0.0730	∠ -83.0

^aSurface concentration of 1-hexadecanol in equivalent monolayers.

^bStirring speed producing the turbulence in rev/min.

Run # 30

Frequency = 0.05 cycles/sec for all data shown below

Type of Reference Chamber (Chamber 1) Clean, Stagnant Surface

Surfactant 1-hexadecanol

	Reference Chamber	Test Chamber
Liquid Temp. (°C)	23.5	24.1
Gas Space Height (cm)	3.175	2.86

Surface Conditions	Comparison of Stagnant and Indicated Surface (Measured Signal)		Comparison of Impermeable and Indicated Surface (Calculated Signal)	
		$(\hat{p}_1 - \hat{p}_2)/\hat{p}_2$		$(\hat{p}_I - \hat{p})/\hat{p}$
stagnant, 0.5 ^a	0.00939	∠ -5.4	0.0331	∠ -55.5
turbulent-150 ^b , 0.5	0.0480	∠ -104.7	0.0772	∠ -79.3
stagnant, 0.5	0.00926	∠ -5.5	0.0332	∠ -55.3
turbulent-230, 0.5	0.101	∠ -99.5	0.131	∠ -86.5
stagnant, 0.5	0.00870	∠ -5.9	0.0335	∠ -54.5
stagnant, 1.0	0.0144	∠ -13.4	0.0283	∠ -60.4
turbulent-150, 1.0	0.0500	∠ -105.1	0.0788	∠ -80.3
stagnant, 1.0	0.0142	∠ -13.5	0.0284	∠ -60.0
turbulent-230, 1.0	0.102	∠ -99.5	0.132	∠ -86.6
stagnant, 1.0	0.0138	∠ -13.6	0.0287	∠ -59.4
stagnant, 2.0	0.0155	∠ -11.2	0.0280	∠ -62.8
turbulent-150, 2.0	0.0505	∠ -105.1	0.0792	∠ -80.5
stagnant, 2.0	0.0147	∠ -11.4	0.0285	∠ -61.5
turbulent-230, 2.0	0.0995	∠ -99.5	0.129	∠ -86.4

^aSurface concentration of 1-hexadecanol in equivalent monolayers.^bStirring speed producing the turbulence in rev/min.

Run # 31-32

Type of Reference Chamber (Chamber 1)	Impermeable Surface
Surface Conditions of Test Chamber (Chamber 2)	Clean, Stagnant Surface
Surfactant	None

	<u>Reference Chamber</u>	<u>Test Chamber</u>
Liquid Temp. (°C)	25.9	26.1
Gas Space Height (cm)	3.175	2.86

Frequency cycles/sec	Comparison of an Impermeable and Clean, Stagnant Surface (Measured Signal)	
	$(\hat{p}_I - \hat{p}_s) / \hat{p}_s$	

0.03	0.05249	∠ -49.98
0.06	0.03594	∠ -48.58
0.10	0.02731	∠ -46.21
0.20	0.02124	∠ -43.86
0.50	0.01349	∠ -45.62
1.00	0.00929	∠ -44.53
2.00	0.00669	∠ -44.61
3.00	0.00520	∠ -47.41

Run # 33-34

Type of Reference Chamber (Chamber 1)	Clean, Stagnant Surface
Surface Conditions of Test Chamber (Chamber 2)	Turbulent, 150 rpm stirring speed
Surfactant	0.0001635-M sodium lauryl sulfonate

	<u>Reference Chamber</u>	<u>Test Chamber</u>
Liquid Temp. (°C)	25.8	26.1
Gas Space Height (cm)	3.175	2.86

Frequency cycles/sec	Comparison of Stagnant and Turbulent Surface (Measured Signal)		Comparison of Impermeable and Turbulent Interface (Calculated Signal)	
	$(\hat{p}_1 - \hat{p}_2)/\hat{p}_2$		$(\hat{p}_I - \hat{p}_t)/\hat{p}_t$	
0.05	0.0416	∠ -105.0	0.0712	∠ -77.0
0.07	0.0280	∠ -114.6	0.0511	∠ -77.3
0.10	0.0174	∠ -113.8	0.0383	∠ -71.0
0.20	0.00639	∠ -117.3	0.0228	∠ -60.9
0.50	0.00151	∠ -120.2	0.0132	∠ -51.5
1.00	0.00067	∠ -113.7	0.00924	∠ -49.0

Run # 33-34

Type of Reference Chamber (Chamber 1)	Clean, Stagnant Surface
Surface Conditions of Test Chamber (Chamber 2)	Turbulent, 230 rpm stirring speed
Surfactant	0.0001635-M sodium lauryl sulfonate

	<u>Reference Chamber</u>	<u>Test Chamber</u>		
Liquid Temp. (°C)	25.8	26.1		
Gas Space Height (cm)	3.175	2.86		
Frequency cycles/sec	Comparison of Stagnant and Turbulent Surface (Measured Signal) $(\hat{p}_1 - \hat{p}_2)/\hat{p}_2$		Comparison of Impermeable and Turbulent Interface (Calculated Signal) $(\hat{p}_I - \hat{p}_t)/\hat{p}_t$	
0.05	0.0723	∠ -105.4	0.0997	∠ -86.4
0.07	0.0463	∠ -104.0	0.0706	∠ -80.9
0.10	0.0311	∠ -103.4	0.0522	∠ -76.8
0.20	0.0132	∠ -102.1	0.0294	∠ -67.8
0.50	0.00388	∠ -91.5	0.0156	∠ -55.7
1.00	0.0223	∠ -74.4	0.0110	∠ -50.9

Run # 36

Type of Reference Chamber (Chamber 1)	Clean, Stagnant Surface
Surface Conditions of Test Chamber (Chamber 2)	Turbulent, 150 rpm stirring speed
Surfactant	0.00106-M sodium lauryl sulfonate

	<u>Reference Chamber</u>	<u>Test Chamber</u>
Liquid Temp. (°C)	25.9	26.2
Gas Space Height (cm)	3.21	2.86

Frequency cycles/sec	Comparison of Stagnant and Turbulent Surface (Measured Signal)		Comparison of Impermeable and Turbulent Interface (Calculated Signal)	
		$(\hat{p}_1 - \hat{p}_2)/\hat{p}_2$		$(\hat{p}_I - \hat{p}_t)/\hat{p}_t$
0.05	0.0279	∠ -116.4	0.0557	∠ -74.6
0.10	0.0111	∠ -119.6	0.0331	∠ -64.6
0.20	0.00411	∠ -120.5	0.0214	∠ -56.0
0.30	0.00235	∠ -120.7	0.0171	∠ -52.9
0.50	0.0012	∠ -117.5	0.0131	∠ -50.2

LEGAL NOTICE

This report was prepared as an account of Government sponsored work. Neither the United States, nor the Commission, nor any person acting on behalf of the Commission:

- A. Makes any warranty or representation, expressed or implied, with respect to the accuracy, completeness, or usefulness of the information contained in this report, or that the use of any information, apparatus, method, or process disclosed in this report may not infringe privately owned rights; or*
- B. Assumes any liabilities with respect to the use of, or for damages resulting from the use of any information, apparatus, method, or process disclosed in this report.*

As used in the above, "person acting on behalf of the Commission" includes any employee or contractor of the Commission, or employee of such contractor, to the extent that such employee or contractor of the Commission, or employee of such contractor prepares, disseminates, or provides access to, any information pursuant to his employment or contract with the Commission, or his employment with such contractor.

TECHNICAL INFORMATION DIVISION
LAWRENCE RADIATION LABORATORY
UNIVERSITY OF CALIFORNIA
BERKELEY, CALIFORNIA 94720